Earth's Climate: the Last 550 Myr

OCEAN 355
Prof. Julian Sachs
Lecture Notes #7
Autumn 2008

Where We've Been & Where We Will Go

- Reviewed what processes control CO_2 greenhouse effect over geologic time (I.e., geochem C cycle).
- And what negative feedbacks (e.g., T-weathering, CO_2-weathering) might keep climate system from reaching &/or remaining in extreme states (e.g., Venus).
- But data (geologic evidence) to support the theory (strong control of climate by CO_2) is lacking*.
- Now turn to geologic evidence for CO_2-climate link during last 500 Myr.

* Prior to ~550 Ma the lack of animals with hard skeletons & vascular plants results in little or no fossil evidence of atmospheric CO_2 levels.

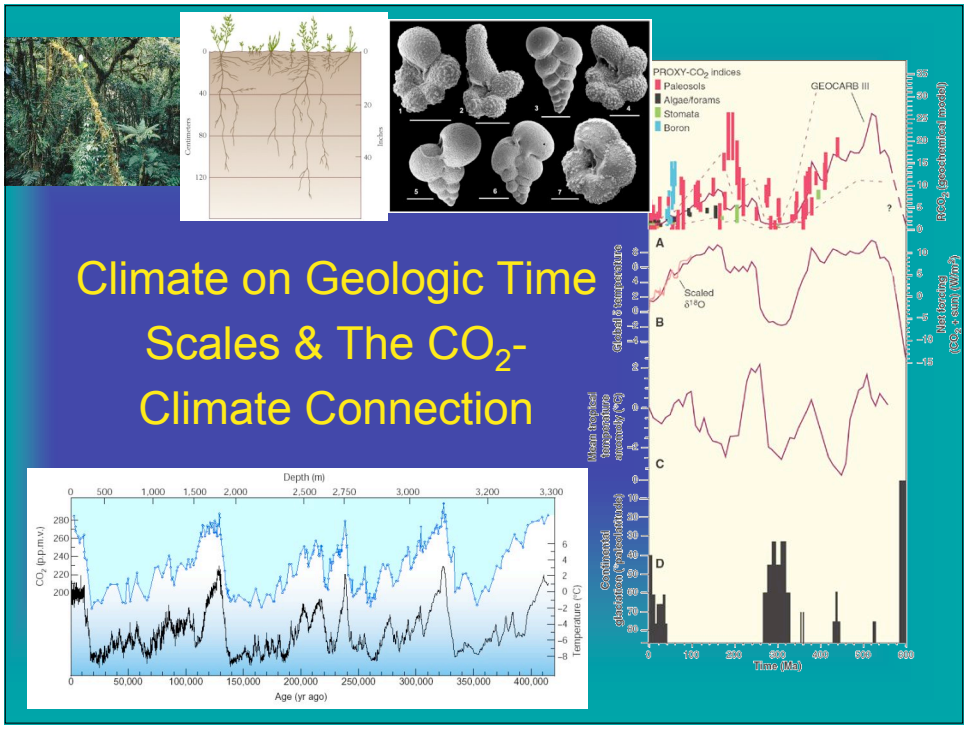

Climate Controls - Long & Short Timescales

- Solar output (luminosity): 10^9 yr
- Continental drift (tectonics): 10^8 yr
- Orogeny (tectonics): 10^7 yr
- Orbital geometry (Earth -Sun distance): 10^4-10^5 yr
- Ocean circulation (geography, climate): 10^1 -10^3 yr
- Composition of the atmosphere (biology, tectonics, volcanoes): 10^0-10^5 yr

Chemical Weathering = chemical attack of rocks by dilute acid

$$CO_2 + H_2O \leftrightarrow H_2CO_3$$

The Geochemical (or non-biological part of the) Carbon Cycle

1. Carbonate Weathering:

$$CaCO_3 + H_2CO_3 \rightarrow Ca^{2+} + 2\,HCO_3^-$$

Carbonate Rocks (e.g., limestone)

2. Silicate Weathering:

$$CaSiO_3 + 2\,H_2CO_3 \rightarrow Ca^{2+} + 2HCO_3^- + SiO_2 + H_2O$$

Silicate Rocks (most of the mantle & crust. E.g., granite)

- 2x CO_2 consumption for silicates
- Carbonates weather faster than silicates

http://en.wikipedia.org/wiki/Image:Yosemite_20_bg_090404.jpg http://en.wikipedia.org/wiki/Image:Burren_karst.jpg

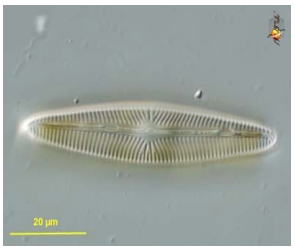

Diatom (SiO_2)

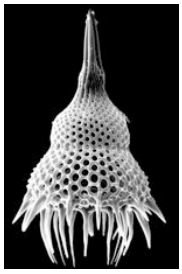

Radiolarian (SiO_2)

Products of weathering precipitaed as $CaCO_3$ & SiO_2 in ocean

R, Protozoans
L, Eukaryotic Phytoplankton

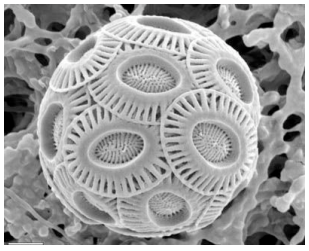

Coccolithophorid ($CaCO_3$)

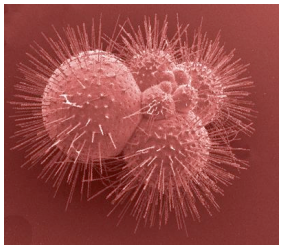

Foraminifer ($CaCO_3$)

Net Reaction of Rock Weathering

+

Carbonate and Silica Precipitation in Ocean

$CaSiO_3 + CO_2 \rightarrow CaCO_3 + SiO_2$

- CO_2 consumed (~ 0.03 Gt C/yr)
- Would deplete atmospheric CO_2 in 20 kyr
- Plate tectonics returns CO_2 via Volcanism and Metamorphism

---

Carbonate Metamorphism

$CaCO_3 + SiO_2 \rightarrow CaSiO_3 + CO_2$

- CO_2 produced from subducted marine sediments

Net reaction of geochemical carbon cycle (Urey Reaction)

- On geologic time scales, rock weathering balanced by carbonate metamorphism
- Any *imbalance* can cause changes in atmospheric CO_2

Carbonate-Silicate Geochemical Cycle

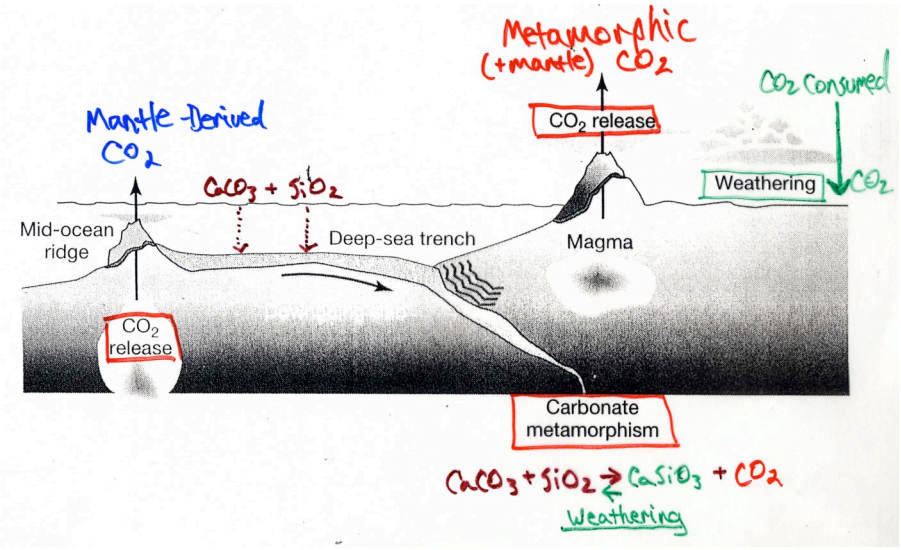

Kump et al. (1999)

- Geologic record indicates climate has rarely reached or maintained extreme Greenhouse or Icehouse conditions....
- Negative feedbacks between climate and Geochemical Carbon Cycle must exist
- Thus far, only identified for Carbonate-Silicate Geochemical Cycle:

  Temp., rainfall enhance weathering rates

  (Walker et al, 1981)

  (I.e., no obvious climate dependence of tectonics or organic carbon geochemical cycle.)

How are CO_2 levels kept in balance?

Feedbacks

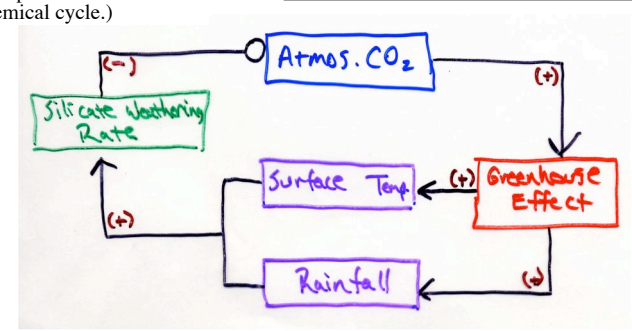

Adapted from Kump et al. (1999)

The CO_2-Climate Connection

→Facts:
- Trace atmospheric gas that efficiently traps outgoing IR

→Hypotheses and theories:
- Solution to FYSP
- Through influence on CO_2: weathering, tectonics and organic carbon burial/oxidation control climate on geologic timescales
- Negative feedbacks:
  1. Temp. – Weathering
  2. CO_2 - Weathering

→Tests:
- Comparisons between "proxies" for CO_2 and T

→State of the science:
- Substantial support for close link… with notable exceptions….

Earth's Surface Radiation Spectrum @ Top of Troposphere

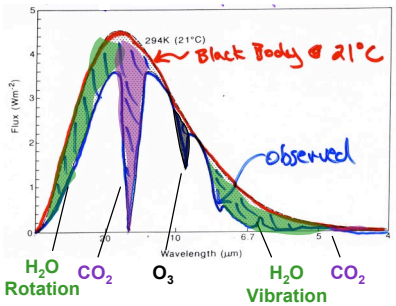

Adapted from Bigg (1996)

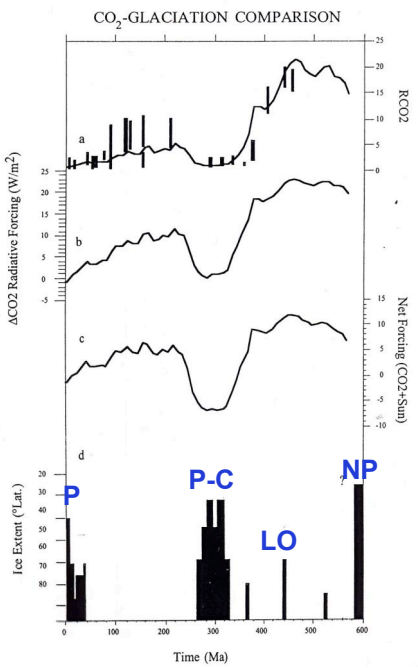

Atmospheric CO_2 During the Phanerozoic Eon (542-0 Ma)

Low (CO_2+S) = Glaciation?

Figure 14.1. (a) Comparison of CO_2 concentrations from a geochemical model (Berner, 1994) with a compilation (Berner, 1997) of proxy CO_2 estimates (vertical bars). CO_2 (b) and solar radiative (c) forcing effects (W m^{-2}) as discussed in the text. Glaciological evidence for continental-scale glaciation (d) from Crowley (1998), which in turn was modified from a compilation from many sources. See text for further discussion.

Crowley (2000)

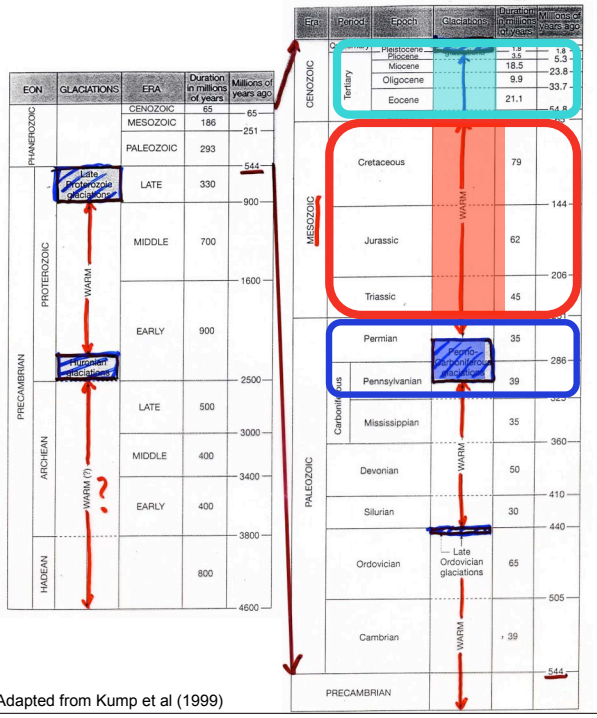

Adapted from Kump et al (1999)

Geologic Evidence for a CO_2-Climate Connection: *Case Studies*

Permo-Carboniferous Glaciations

Mesozoic Warmth

Cenozoic Cooling

Permo-Carboniferous Glaciations (~300-275 Ma)

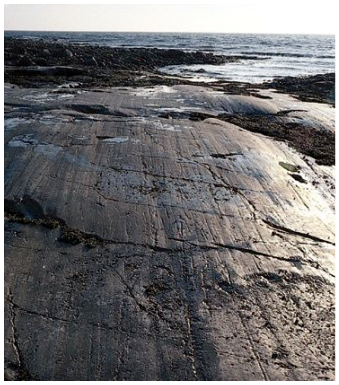

Stanley (2000)

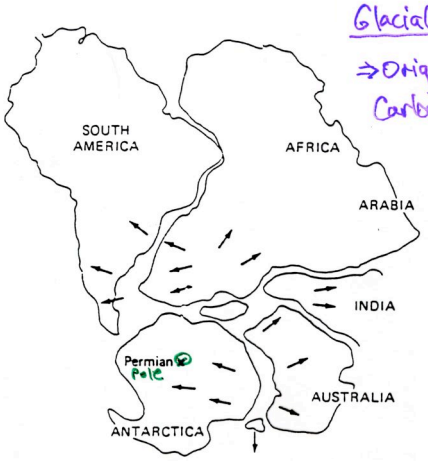

Glacial striations
⇒ Origin of Permo-Carboniferous Glaciation
COLD

Fig. 11.11. Generalized diagram illustrating evidence for origination of Permo-Carboniferous glaciation on one large landmass. Arrows indicate direction of glacial flow. X = Permian pole position. [After Sullivan, 1974] *Reproduced by permission from W. Sullivan, "Continents in Motion: The New Earth Debate," copyright 1974, McGraw-Hill Publishing Co.*

Phanerozoic CO_2 Evolution

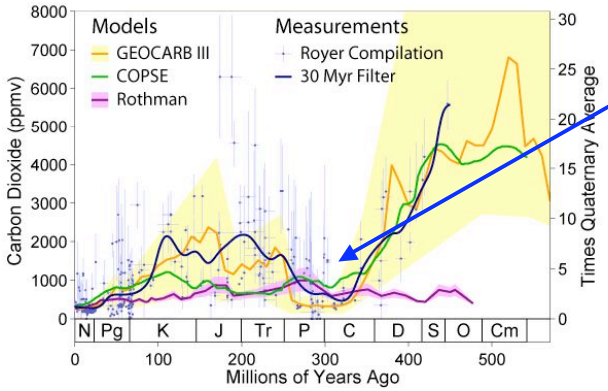

• Permo-Carboniferous Glaciations Followed a period of marked CO_2 decline

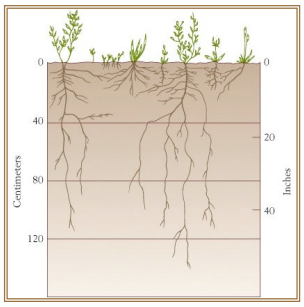

Stanley (2000)

• CO_2 decline likely resulted from spread of rooted vascular plants in the Devonian, 400-360 Ma.
• Dissolution of bedrock (weathering) from: secreted acids, metabolic CO_2 from C_{org} decomposition, & anchoring of clay-rich soil to rock (which retains water).

Theory: Berner (1997) *Science*, Vol. 276: 544-547
http://www.globalwarmingart.com/wiki/Image:Phanerozoic_Carbon_Dioxide_png.

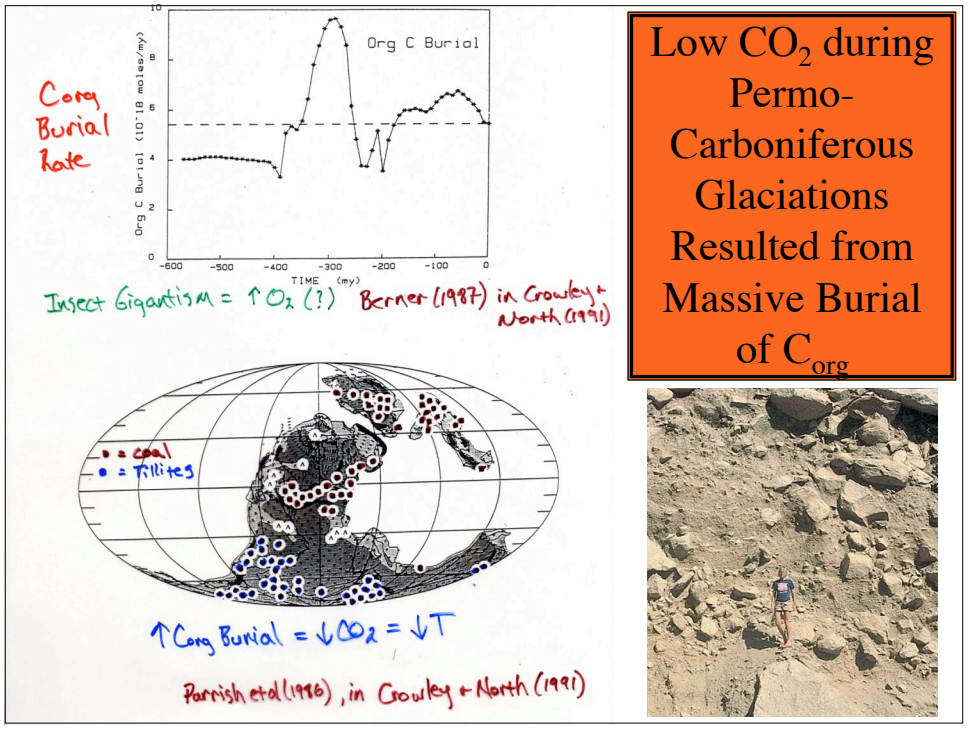
Org C Burial
Org C Burial (10^18 moles/my)
TIME (my)
Corg Burial Rate
Insect Gigantism = ↑O2 (?) Berner (1987) in Crowley + North (1991)
= coal
= Tillites
↑Corg Burial = ↓CO2 = ↓T
Parrish et al (1986), in Crowley + North (1991)
Low CO2 during Permo-Carboniferous Glaciations Resulted from Massive Burial of Corg

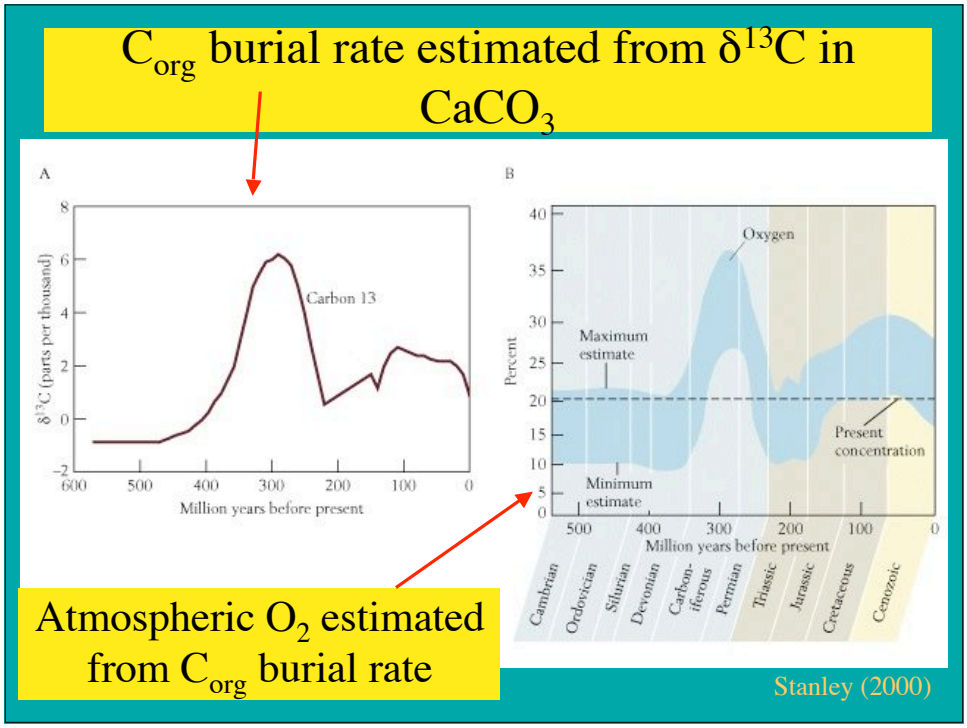
Corg burial rate estimated from δ13C in CaCO3
A
δ13C (parts per thousand)
Carbon 13
Million years before present
B
Percent
Oxygen
Maximum estimate
Minimum estimate
Present concentration
Million years before present
Cambrian
Ordovician
Silurian
Devonian
Carbon-iferous
Permian
Triassic
Jurassic
Cretaceous
Cenozoic
Atmospheric O2 estimated from Corg burial rate
Stanley (2000)

High C_{org} Burial Results in High $^{13}C/^{12}C$ in Seawater & $CaCO_3$

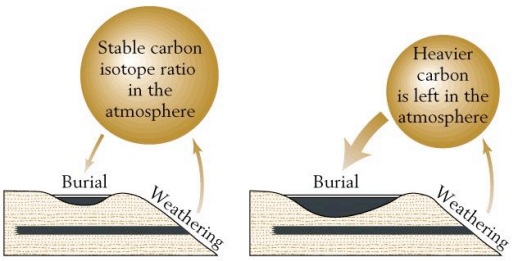

A Burial rate of carbon balances weathering rate

B Burial rate of carbon exceeds weathering rate

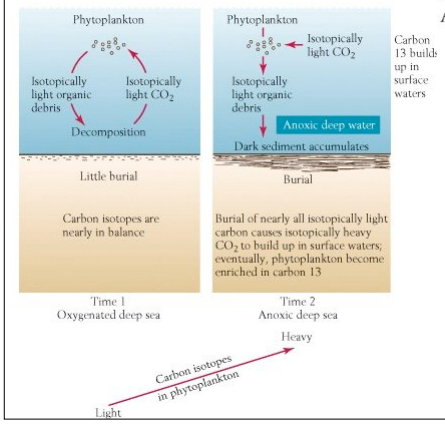

On longer time scales, higher burial rates of C, relative to weathering rates, results in elevated $^{13}C/^{12}C$ in atmos/ocean

Stanley (2000)

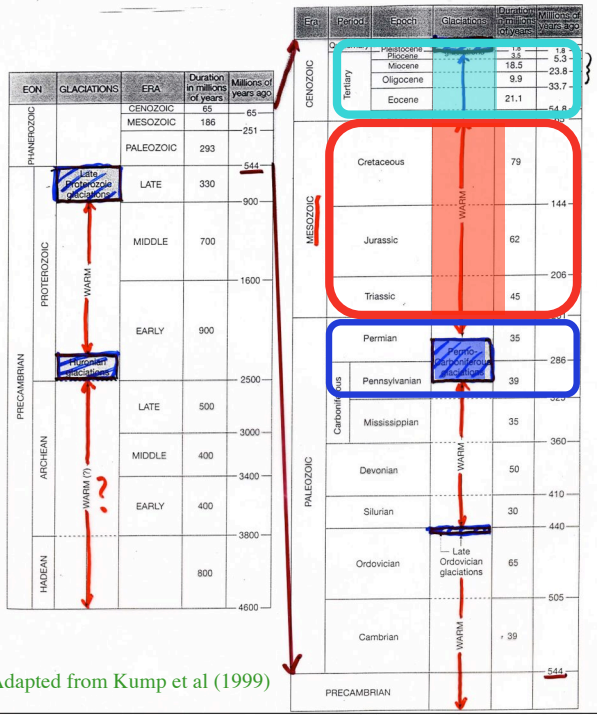

Adapted from Kump et al (1999)

Geologic Evidence for a CO_2-Climate Connection: *Case Studies*

Permo-Carboniferous Glaciations

Mesozoic Warmth

Cenozoic Cooling

Mesozoic Warmth

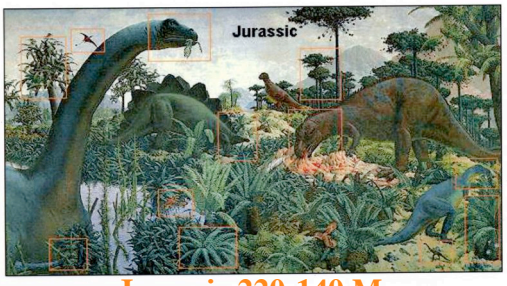

Jurassic 220-140 Ma

Cretaceous 140-65 Ma

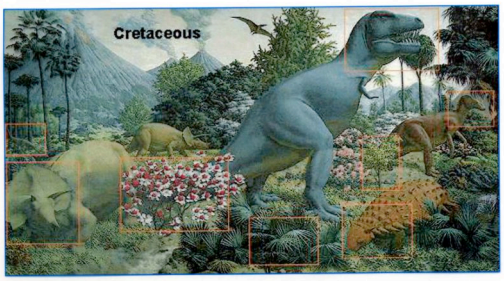

•Ferns & alligators in Siberia
•Dinosaur bones in AK (N of Arctic Circle)

Stanley (2000)

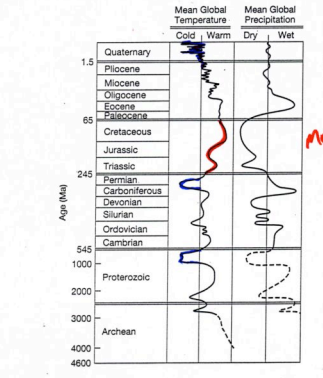

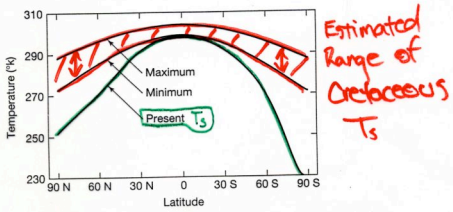

FIGURE 8-15
Estimated limits on longitudinally averaged surface temperatures during the mid-Cretaceous period, 100 m.y. ago, as compared with today. (After E. J. Barron and W. M. Washington, "The Carbon Cycle and Atmospheric CO_2," *Geophysical Monograph* 32, AGU, Washington, D.C., 1985.)

20°-60° Warmer at Poles!

2°-6° Warmer at Equator

Decreased Equator-to-Pole Temperature Gradient

Kump et al. (1999)

High CO_2 Levels During Mesozoic

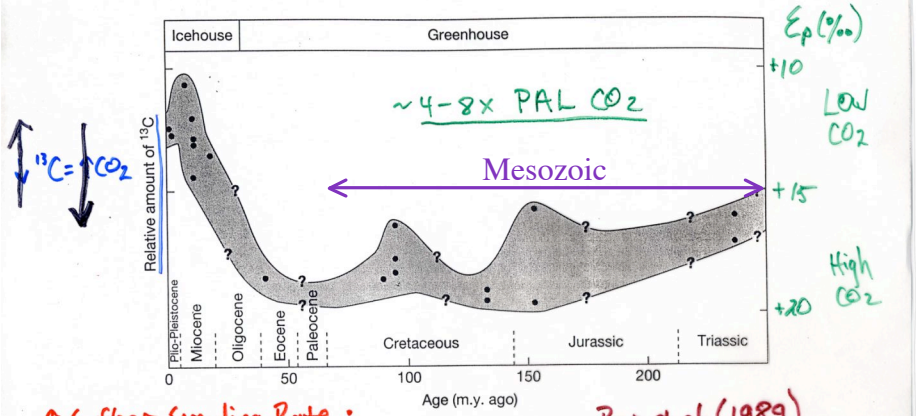

↑ Seafloor Spreading Rate:

(1) ↑ CO_2 outgassing

(2) ↑ Subduction Rate = ↑ Carbonate Metamorphism = ↑ CO_2 Production

(3) ↑ Sea Level (Hotter Oceanic Crust / Higher Ridge Volume) = ↓ Land Area = ↓ Weathering = ↓ CO_2 Sink

Popp et al. (1989)

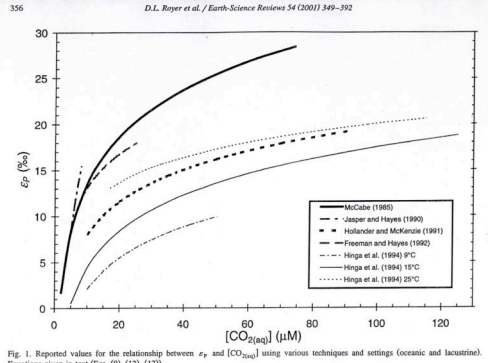

Fig. 1. Reported values for the relationship between ε_p and $[CO_{2(aq)}]$ using various techniques and settings (oceanic and lacustrine). Equations given in text (Eqs. (9), (12)–(17)).

$$\varepsilon_p \equiv \varepsilon_{diff} + (\varepsilon_f - \varepsilon_{diff}) \times \frac{C_{int.}}{C_{ext.}}$$

$$\varepsilon_p = 0.7 + 24.3 \times \frac{C_{internal}}{C_{external}}$$

$\varepsilon_f \cong 27$ ‰ Land Plants

$\cong 25$ ‰ Phytoplankton

$\varepsilon_{diff} = 0.7$ ‰

Paleo *p*CO2 Estimates from Carbon Isotopic Fractionation by Algae

Royer et al. (2001)

Carbon Isotopic Fractionation Indicates pCO_2

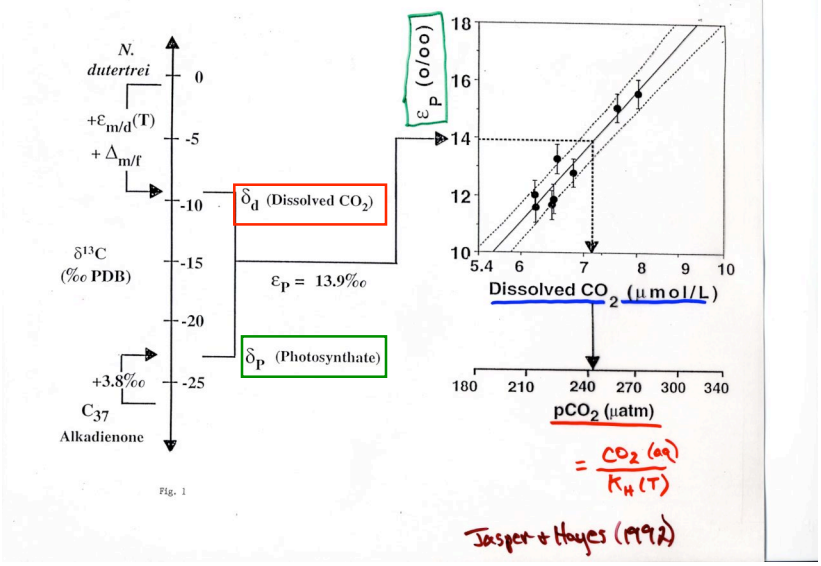

Seafloor Spreading Rates Appear to have Been High in Latter Half of Mesozoic

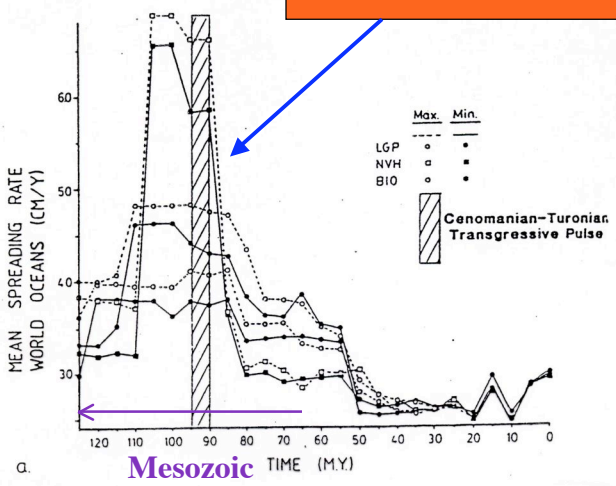

- High seafloor spreading rates provide potential source of elevated CO_2

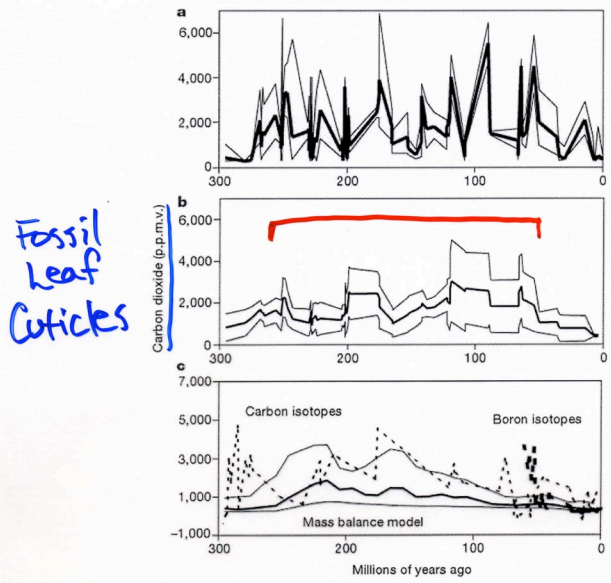

Fossil Leaf Cuticles

Fossil leaf cuticles provide evidence for elevated CO_2 during Mesozoic

3-6 x PAL during Mesozoic

SI(%)=SD/(SD+ED)*100%

SD= stomatal density
ED=epidermal cell density

(I.e., the proportion of epidermal cells that are stomata

Retallack (2001), *Nature* , Vol. 411, pp. 287-290

CO_2 from Leaf Stomatal Indices

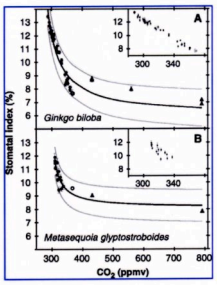

Royer et al (2001), *Science* , Vol. 292, pp. 2310-2313

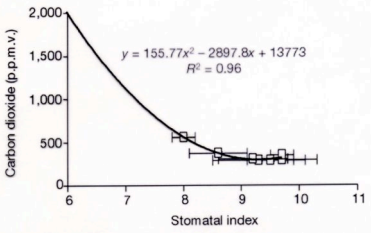

Retallack (2001), *Nature* , Vol. 411, pp. 287-290

Calibrating the Leaf Stomatal "Paleo-barometer"

Extrapolation to high pCO_2 not (yet) supported by data…

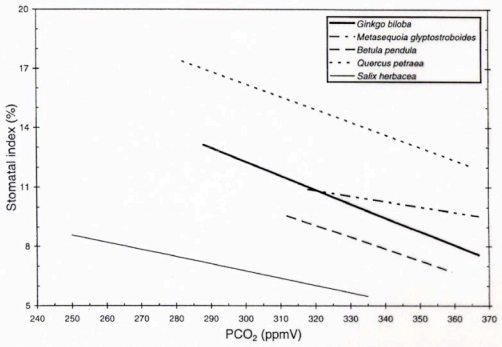

Fig. 9. Stomatal index response of five species to PCO_2. Data compiled from herbarium sheets and altitudinal transects. Sources are as follows: *Ginkgo biloba* and *Metasequoia glyptostroboides* (Royer, unpublished data); *Betula pendula* (Wagner et al., 1996); *Quercus petraea* (Kürschner et al., 1996); *Salix herbacea* (Rundgren and Beerling, 1999).

Royer et al. (2001)

Response of stomata to [CO_2] is species-dependent

Limiting SI-derived paleo-CO_2 estimates to times and places when fossilized leaves from extant species exist…

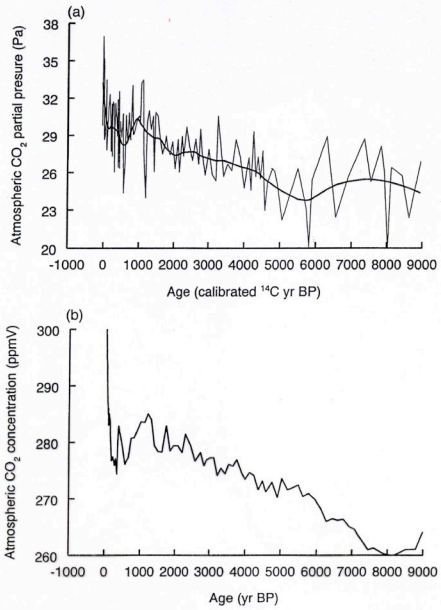

Fig. 12. Holocene reconstructed variations in (a) the partial pressure of atmospheric CO_2 using fossil *Salix herbacea* leaves (after Rundgren and Beerling, 1999) and (b) measurements of atmospheric CO_2 from ice cores (after Indermühle et al., 1999b).

Nevertheless, calibrations of the SI appear accurate for at least the last 9 kyr

Royer et al. (2001)

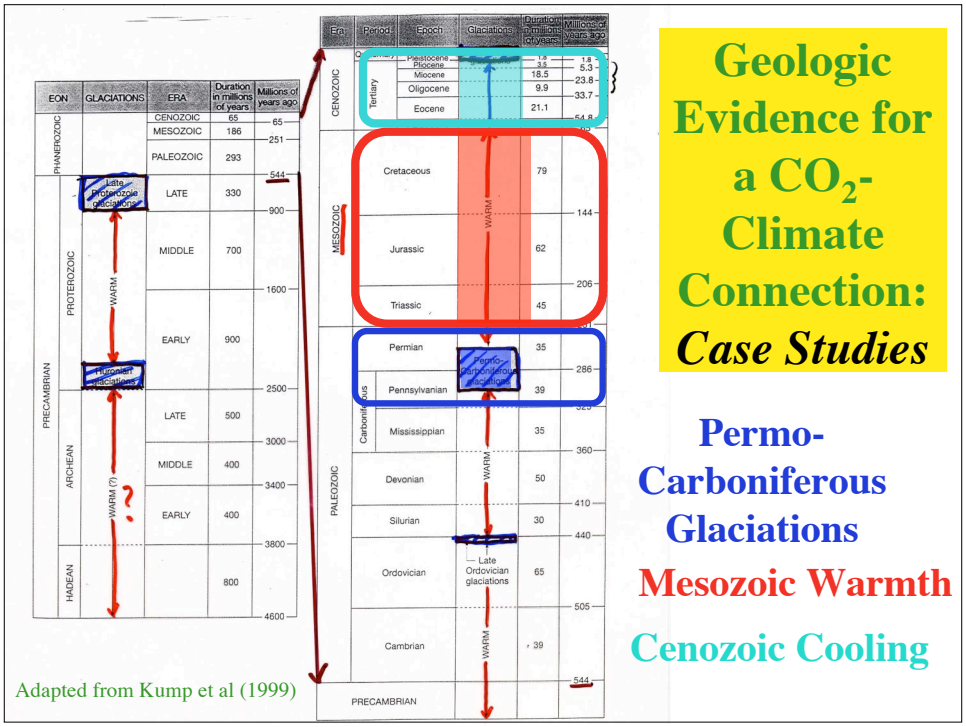
Geologic Evidence for a CO_2-Climate Connection:
Case Studies
Permo-Carboniferous Glaciations
Mesozoic Warmth
Cenozoic Cooling
Adapted from Kump et al (1999)

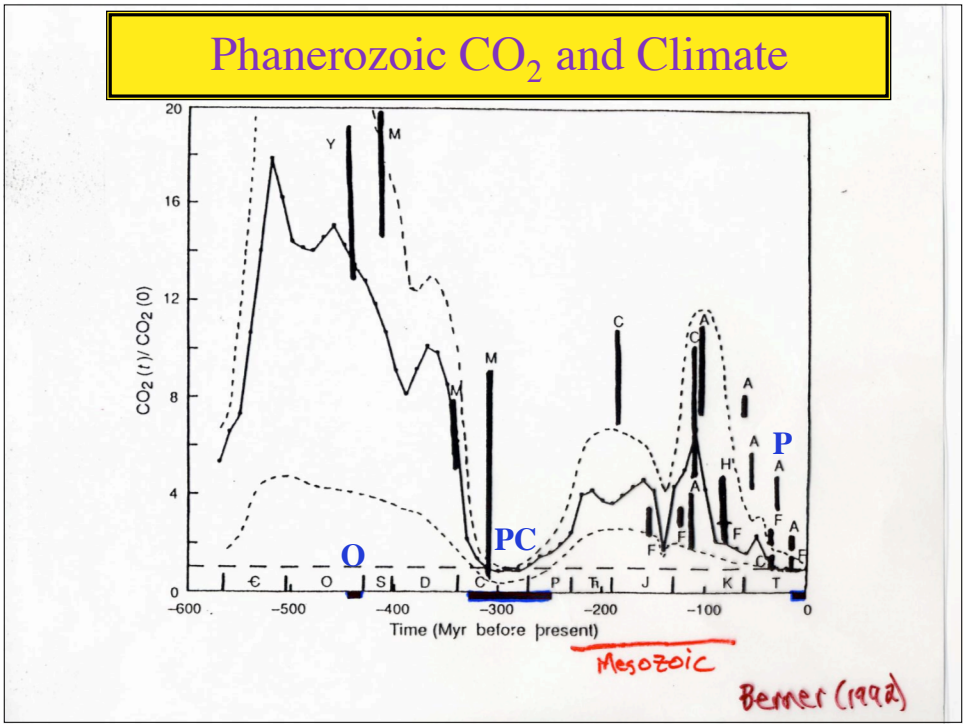
Phanerozoic CO_2 and Climate
CO_2 (t) / CO_2 (0)
Time (Myr before present)
PC
O
P
Mesozoic
Berner (1992)

Cenozoic CO_2 Decrease

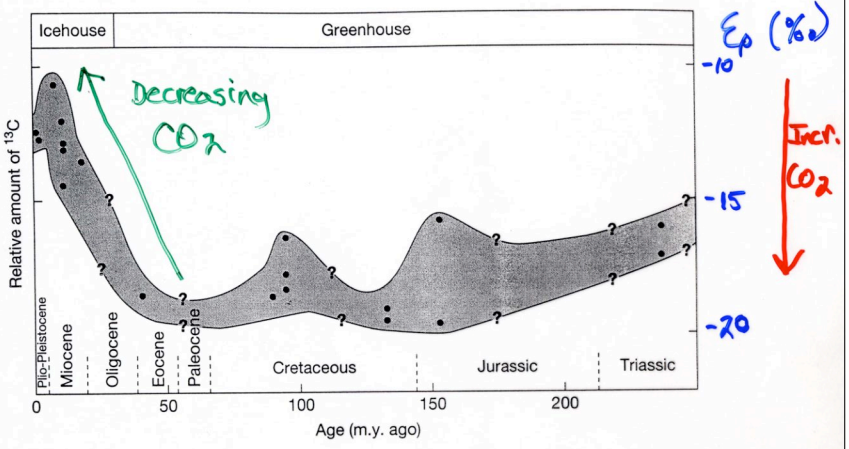

Popp et al. (1989)

Carbon Isotopic Fractionation Indicates pCO_2

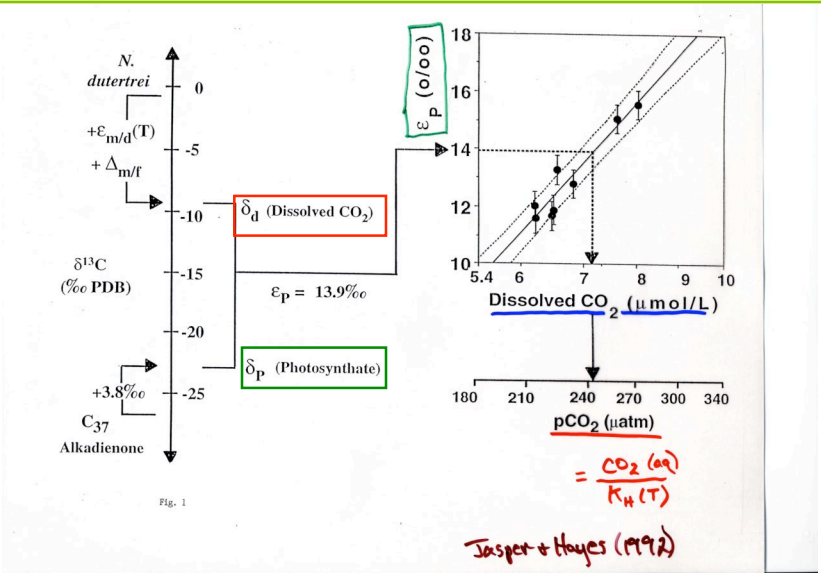

Jasper & Hayes (1992)

Boron Isotopes in Seawater Also Indicate Large Cenozoic CO_2 Decline

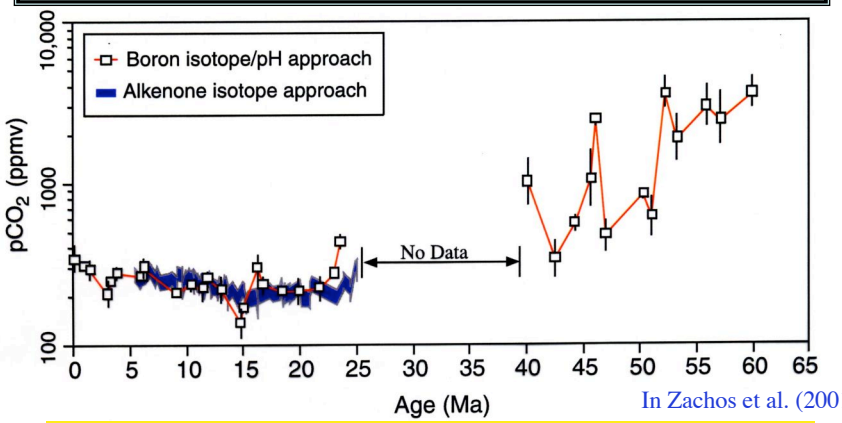

In Zachos et al. (2001)

- B in seawater: $B(OH)_3$, $B(OH)_4^-$
- Relative abundance controlled by *p*H
- B incorporated into calcite: $B(OH)_4^-$
- Strong isotopic fractionation between ^{10}B & ^{11}B:
  ^{10}B = tetrahedral coordination, -19.8‰ relative to ^{11}B

$\delta^{11}B = [(^{11}B/^{10}B)_{smpl} / (^{11}B/^{10}B)_{std} - 1] \times 1000‰$

Cenozoic Cooling 80-0 Ma

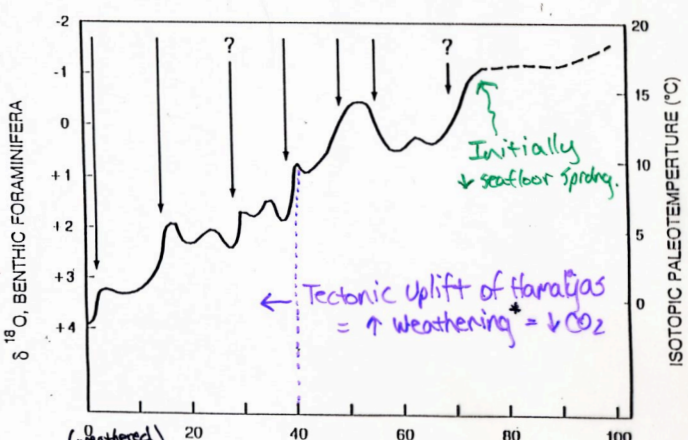

* Fresh, easily erodable silicates
* Orographic concentration of rain on mtns.
* Steep slopes to rapidly flush weathering products

After Raymo et al. (1988, 1991, 1992)

Declining Seafloor Spreading Rates 80-40 Ma

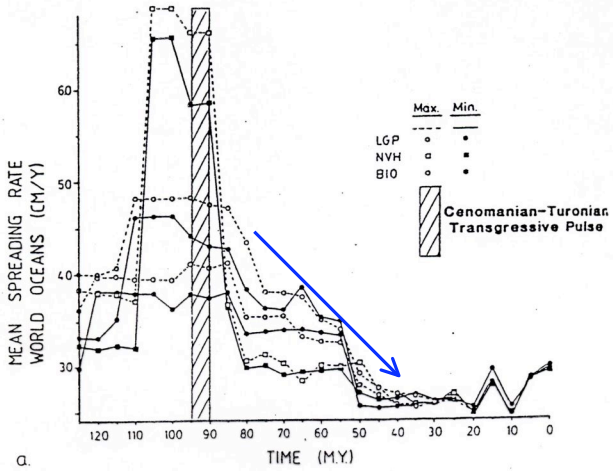

•Declining s.f. spreading rates are consistent with decreasing CO_2 in early Cenozoic

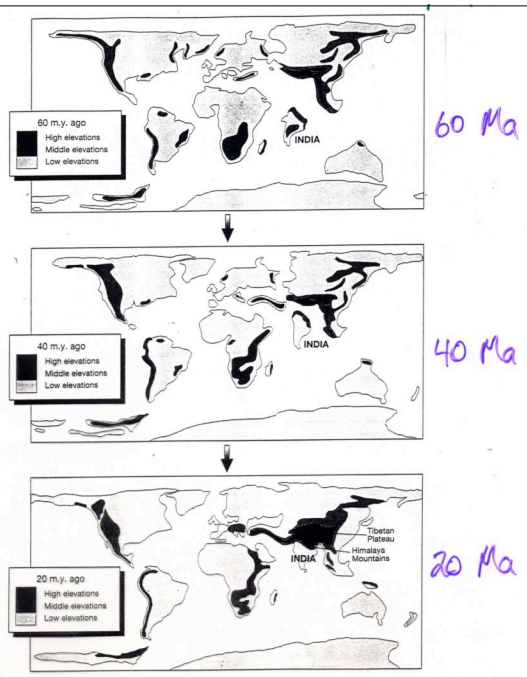

Himalayan Orogeny & Uplift of Tibetan Plateau

Increasing Strontium Isotopic Composition of Seawater During Cenozoic Implies Increasing Weathering Rates

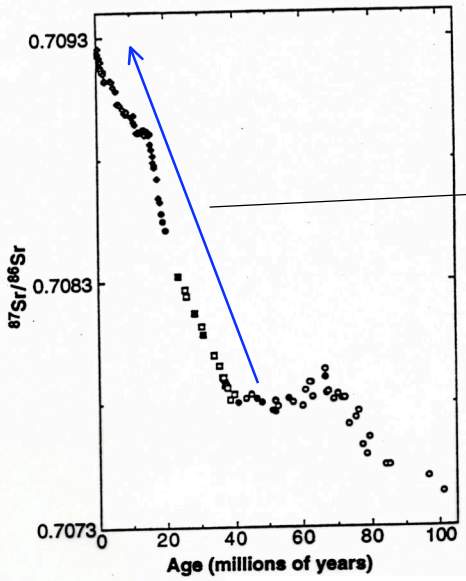

SW $^{87}Sr/^{86}Sr$ is balance between:

1. Deep-sea hydrothermal input of non-radiogenic Sr (0.7035)
2. More radiogenic input riverine flux from continental weathering (0.712)

Abyssal carbonate $^{87}Sr/^{86}Sr$
^{87}Rb-->^{87}Sr, $t_{1/2}$~48 Gyr

DePaolo & Ingram (1985)
in Edmond (1992)

Strontium Isotope Systematics

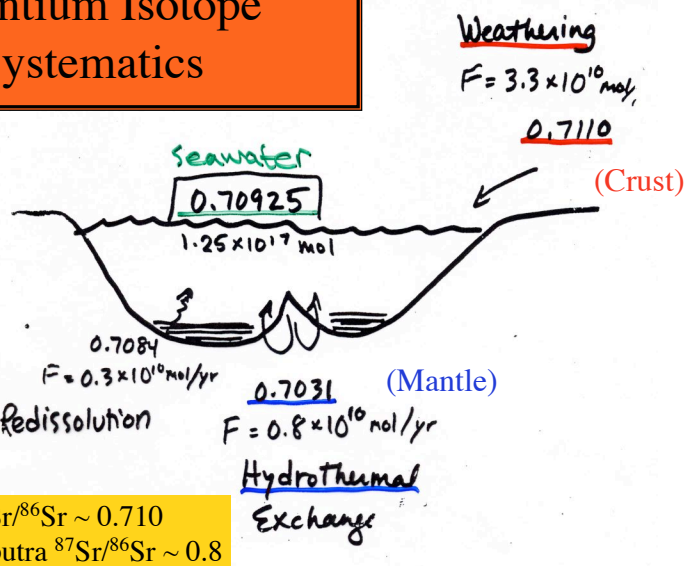

Normal River $^{87}Sr/^{86}Sr$ ~ 0.710
Ganges-Brahmaputra $^{87}Sr/^{86}Sr$ ~ 0.8

Co-Variation of $^{87}Sr/^{86}Sr$ & CO_2 through the Phanerozoic

$\varepsilon_p \sim \varepsilon_{toc} = \delta^{13}C_{CaCO3} - \delta^{13}C_{org}$

$\varepsilon_p \sim pCO_2$

High weathering &/or **Low** magmatism

High CO_2

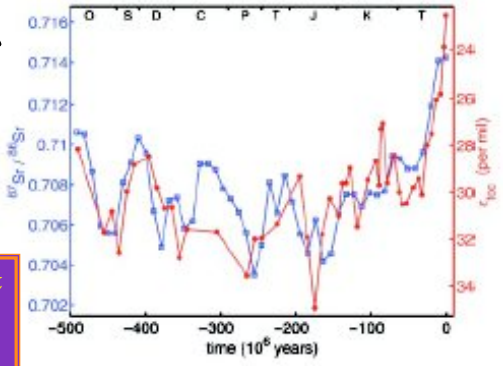

g. 3. The function *g* (blue squares) obtained by removing the memory flux om the $^{87}Sr/^{86}Sr$ data of Fig. 1, along with ε_{toc} (red circles). Note that the nge of the $^{87}Sr/^{86}Sr$ curve is approximately five times greater than in Fig. 1. e data are plotted such that the mean of both time series lies on the same rizontal line and their rms fluctuations have the same vertical extent.

•Weathering & magmatism may control CO_2, but does CO_2 control climate?

Rothman (2002) *PNAS*, Vol 99(7):4167

CO_2 During the last 450 kyr from the Vostok, Antarctica Ice Core

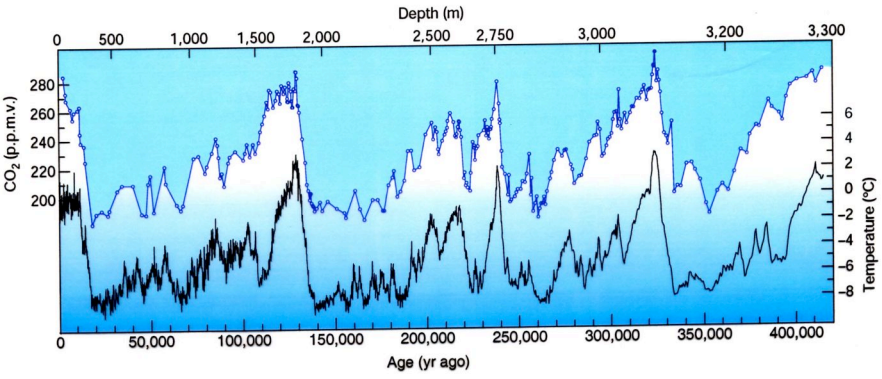

Petit et al (1999) in Kump (2002), *Nature*, vol. 419:188-190.

Covariation Between CO_2 and T in Pleistocene

Vostok Ice Core, Central East Antarctica

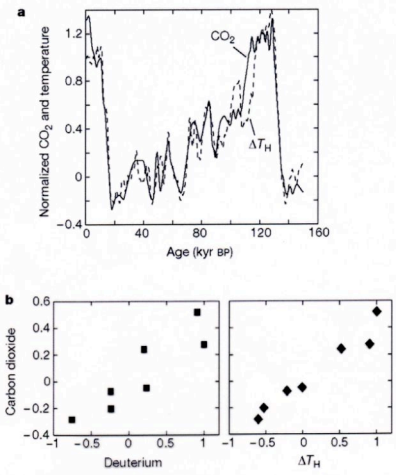

Cuffey and Vimeux (2001), *Nature* , Vol. 412, pp. 523-527

What caused glacial-interglacial CO_2 variations?

(a still-unanswered question!)

Possible Scenario for lower glacial CO_2

- Increased:
  Equator-Pole T gradient, Wind strength, Dust flux to ocean, Iron flux to ocean
- 50% of global 1° production occurs in ocean
- Ocean 1° production is limited by iron
- Higher 1° production draws CO_2 out of atmosphere & sequesters it in the deep ocean & sediments
- Colder seawater dissolves more CO_2

letters to nature

Evidence for decoupling of atmospheric CO_2 and global climate during the Phanerozoic eon

Jan Veizer*, Yves Godderis* & Louis M. François†

* Institut für Geologie, Mineralogie und Geophysik, Ruhr Universität, 44780 Bochum, Germany, and Ottawa-Carleton Geoscience Centre, University of Ottawa, Ottawa, ON K1N 6N5, Canada
† Laboratoire de Physique Atmosphérique et Planétaire, Université de Liège, 4000 Liège, Belgium

Atmospheric carbon dioxide concentrations are believed to drive climate changes from glacial to interglacial modes[1], although geological[2,3] and astronomical[4–6] mechanisms have been invoked as ultimate causes. Additionally, it is unclear[7,8] whether the changes between cold and warm modes should be regarded as a global phenomenon, affecting tropical and high-latitude temperatures alike[9–11], or if they are better described as an expansion and contraction of the latitudinal climate zones, keeping equatorial temperatures approximately constant[9–16]. Here we present a reconstruction of tropical sea surface temperatures throughout the Phanerozoic eon (the past ~550 Myr) from our database[17] of oxygen isotopes in calcite and aragonite shells. The data indicate large oscillations of tropical sea surface temperatures in phase with the cold–warm cycles, thus favouring the idea of climate variability as a global phenomenon. But our data conflict with a temperature reconstruction using an energy balance model that is forced by reconstructed atmospheric carbon dioxide concentrations[18]. The results can be reconciled if atmospheric carbon dioxide concentrations were not the principal driver of climate variability on geological timescales for at least one-third of the Phanerozoic eon, or if the reconstructed carbon dioxide concentrations are not reliable.

Calculated partial pressures of CO_2 in the atmosphere[19–24] (pCO_2) are indeed relatively low for the Permo/Carboniferous and Cenozoic icehouse episodes[1], times of predominantly cold climates lasting tens of millions of years[1], but for the other two Phanerozoic icehouses—the late Ordovician/earliest Silurian and the late Jurassic/early Cretaceous—all global biogeochemical models[18,20] predict high pCO_2 levels. In an attempt to resolve this discrepancy, particularly for the late Ordovician glaciation(s), theoretical models advocating the development of permanent high-latitude ice sheets[11] at more than 10 times present-day CO_2 levels have been proposed. As an alternative, we present here experimental evidence that suggests large variations in tropical sea surface temperatures (SSTs; up to 9 °C) between the peaks of greenhouse/icehouse modes.

The testing of model predictions on Phanerozoic timescales has been hampered by the lack of high-resolution isotope databases for ancient sea water, as reflected in the chemical sediments. This has been particularly the case for oxygen isotopes, where the depletion in ^{18}O for progressively older sediments was mostly considered to be a product of post-depositional diagenetic overprint. However, new databases have been published[17] recently—based on ~4,500 low-Mg calcitic and 125 aragonitic shells—for $\delta^{18}O$, $\delta^{13}C$ and $^{87}Sr/^{86}Sr$, establishing the baseline for Phanerozoic $\delta^{18}O$ (Fig. 13 in ref. 17). Most studied samples originate from the photic zone of palaeotropical seas (30 °S–30 °N). The entire datasets are available at http://www.science.uottawa.ca/geology/isotope_data. Reference 17, because of the huge number of measurements, dealt only with the documentation of data and their quality, and with the arguments for the primary nature of the $\delta^{18}O$ record.

The secular trend for the $\delta^{18}O$ values of Phanerozoic carbonates, Fig. 13 in ref. 17, consists of a long-term rising linear trend that exceeds the duration of planetary greenhouse/icehouse modes. This trend is tectonically controlled, a proposition supported by the strong correlation of $\delta^{18}O$ with the $^{87}Sr/^{86}Sr$ signal for the Phanerozoic sea water (Figs 16 and 17 in ref. 17). Sr isotopes are a proxy for terrestrial tectonic processes, because seawater $^{87}Sr/^{86}Sr$ is controlled principally by inputs of Sr from rivers (weathering of ^{87}Sr-enriched continental crust) and from hydrothermal circulation cells at mid-ocean ridges (interaction with ^{87}Sr-depleted basalts). Such long-term tectonic signals have to be subtracted from the superimposed higher-order oscillations before any discussion of climatic consequences, and we therefore detrend the data by removing the least-squares linear fit.

The first-order $\delta^{18}O$ oscillations around the least-squares fit correlate well with the palaeoclimate as established from sedimentological criteria[1]. The icehouses usually coincide with ^{18}O-enriched values and greenhouses with ^{18}O-depleted values (Fig. 1). We propose therefore that the Phanerozoic $\delta^{18}O$ oscillations reflect variations in SSTs. Future improvements on the Phanerozoic database may result in amelioration of the amplitudes, or in partial temporal shifts of some of the peaks. This is particularly the case for the Neogene interval, where the running mean is forced to higher values by the inclusion of some isotopically heavy planktonic

Acknowledgements

This research was supported by the NSF Division of Materials Research, and the Petroleum Research Fund administered by the American Chemical Society. We thank M. D. Ediger for helpful discussions and E. Sioutharidiy for assistance.

Correspondence and requests for materials should be addressed to N.E.L. (e-mail: lenaleff@msn.edu).

While a large and growing body of evidence indicates that CO_2 and climate co-vary, there is some indication that the two may not be closely linked at all times….

(& it is always important to remember that *correlation* does not always mean *causation*)

Cool Tropics - High CO_2 (?)

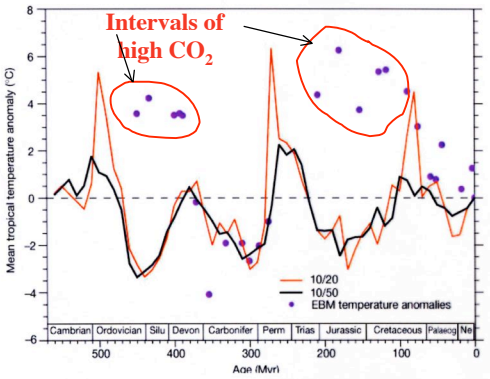

Veizer et al. (2000), *Nature* , Vol. 408, pp. 698-701

(or diagenetic alteration of $CaCO_3$?)

Model-Data SST Comparison

Tropical SST anomaly (Data)
-Assumes 2‰ of 3-5‰ $\delta^{18}O$ range due to ice volume (2x present ice volume in "icehouse"; No ice in "greenhouse").
-Leaves ~2‰, or ~9°C of SST change

Simple E Balance Model
-CO_2 (Berner, 1992)
-Solar constant increasing by 5% over Phanerozoic

$T_s - \Delta T_g = T_{eff}$

$\sigma T_{eff}^4 = S/4*(1-A)$

T-dependent Isotopic Fractionation

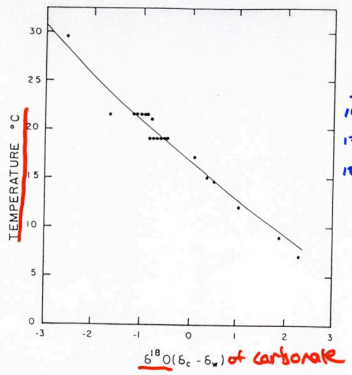

Natural Abundances
^{16}O = 99.756%
^{17}O = 0.039
^{18}O = 0.205

$CaC^{16}O_3 + H_2{}^{18}O \leftrightarrow CaC^{16}O_2{}^{18}O + H_2{}^{16}O$

$T = 16.9 - 4.2(\delta^{18}O_c - \delta^{18}O_w)$

$\delta^{18}O_w = f(\text{Salinity, ice volume})$

$$\delta^{18}O = \left[\frac{(^{18}O/^{16}O)_{sample}}{(^{18}O/^{16}O)_{standard}} - 1\right] \times 1000‰$$

Epstein et al. (1953)

A Temperature-Dependent Isotopic Fractionation of ^{18}O from ^{16}O Occurs During Calcification

$\delta^{18}O$ of Seawater varies w/ Salinity

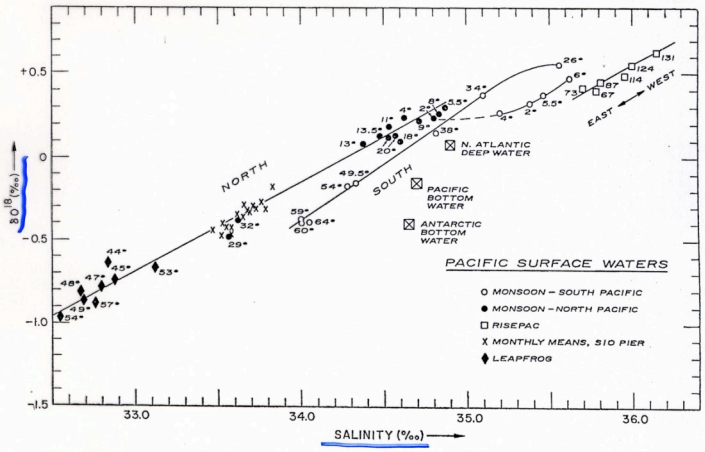

FIGURE 10. — *Oxygen 18-salinity relationships in surface and deep Pacific Ocean samples. Latitudes are shown for Monsoon and Leapfrog samples: the figures on the Risepac expedition points are station numbers shown in figure 6.*

H. Craig and L. I. Gordon (1965)

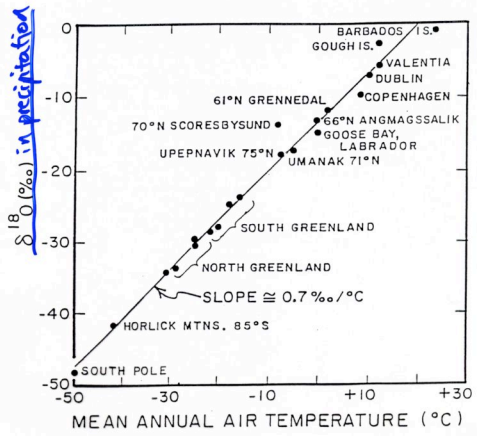

Dansgaard (1964)

- $\delta^{18}O$ of precipitation varies with latitude & altitude.
- Water derived from melting snow & ice is highy depleted in ^{18}O.
- Airmass trajectory influences $\delta^{18}O$ of precipitation

$H_2{}^{18}O$ has 1% lower vapor P

∴ Cold Air (High latitude +/or Altitude) has low $\delta^{18}O$

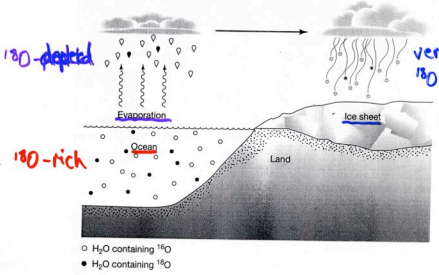

Influence of Ice Volume on Ocean $\delta^{18}O$

1.3‰ Decrease of Ocean $\delta^{18}O$ from Melting Glaciers

120 M Sea Level Depression @ LGM

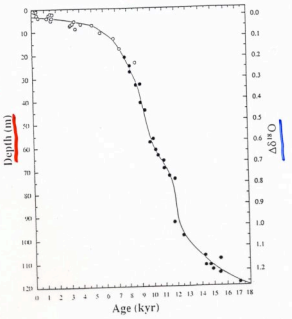

FIG. 2 Barbados sea level curve based on radiocarbon-dated *A. palmata* (filled circles) compared with *A. palmata* age-depth data[4] (open circles) for four other Caribbean island locations. All radiocarbon ages in this figure are corrected for local seawater $\Delta^{14}C$ by subtracting 400 yr from the measured radiocarbon ages[4] but they are not corrected for secular changes in atmospheric ^{14}C levels[15]. The Barbados data are corrected for the estimated mean uplift of 34 cm kyr^{-1}. The right-hand axis of the Barbados sea level curve (solid line) is scaled to the estimated $\delta^{18}O$ change of mean ocean water using the calibration in ref. 5.

Fairbanks (1989), Nature, 342: 637-642

Diagenetic Alteration of $^{18}O/^{16}O$ in $CaCO_3$

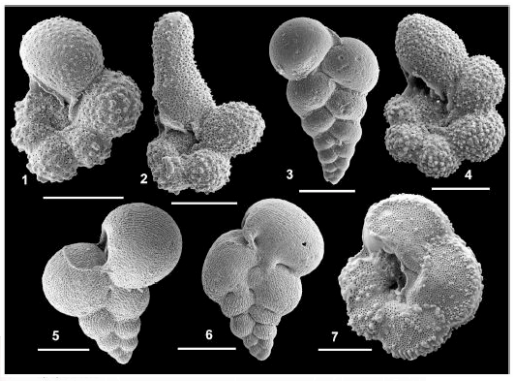

Foraminifera

Photo of *Helenina anderseni*

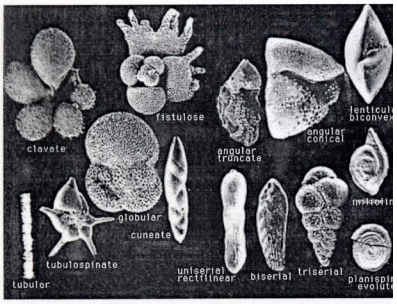

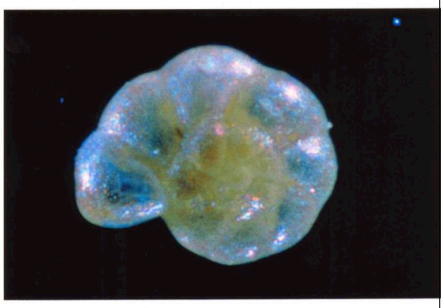

Recrystallization of Foram Calcite

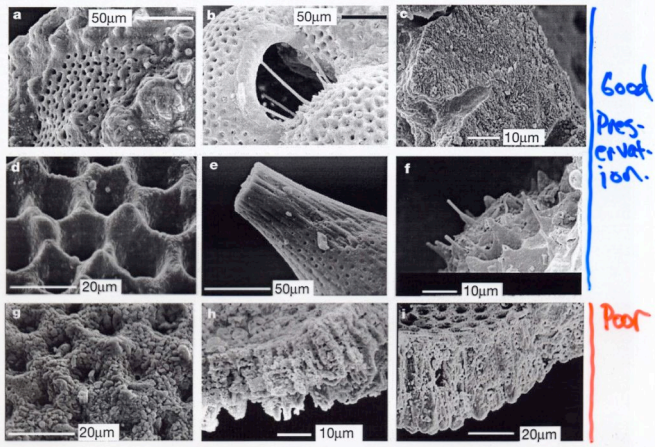

Pearson et al. (2001), Nature, 413: 481-487

Large Effect of Diagenesis Makes T Estimates Biased to Cold

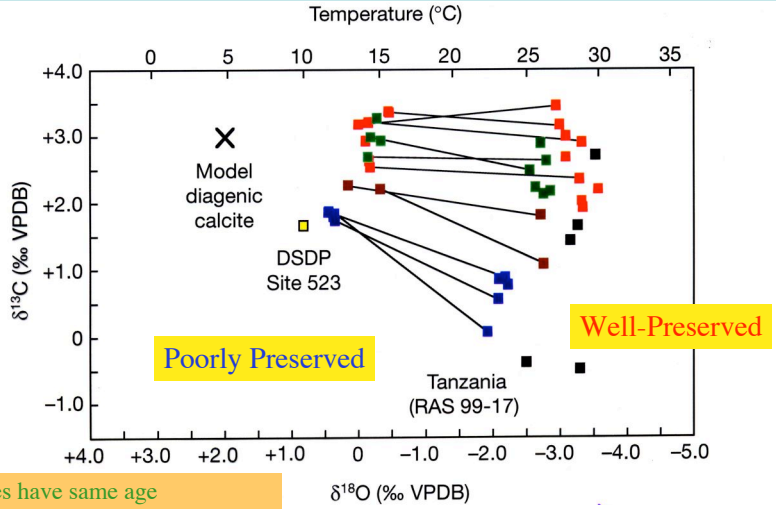

- Samples have same age
- Lines connect same species of foraminifera

Pearson et al. (2001) *Nature* Vol. 413: 481-487.

Well-Preserved Forams Indicate ↑Tropical SST

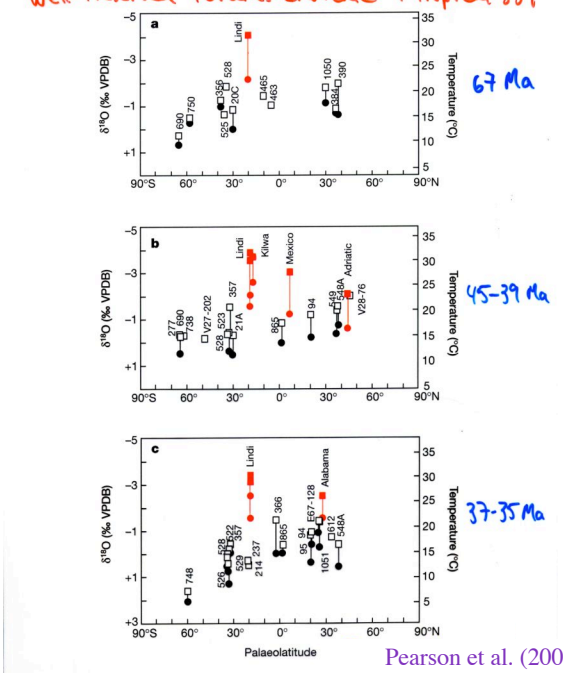

67 Ma

45-39 Ma

37-35 Ma

Well-Preserved Fossils are Essential!

Pearson et al. (2001) *Nature* Vol. 413: 481-487.

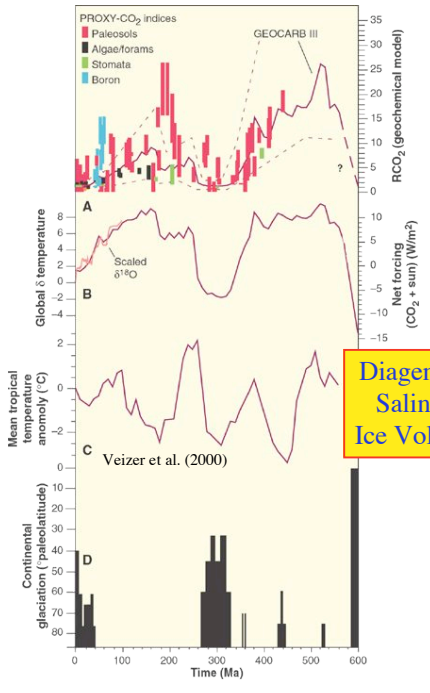

Diagenesis?
Salinity?
Ice Volume?

CO_2 & Climate

Records of change. **(A)** Comparison of CO_2 concentrations from the GEOCARB III model (6) with a compilation (9) of proxy-CO_2 evidence (vertical bars). Dashed lines: estimates of uncertainty in the geochemical model values (6). Solid line: conjectured extension to the late Neoproterozoic (about 590 to 600 Ma). RCO2, ratio of CO_2 levels with respect to the present (300 parts per million). Other carbon cycle models (21, 22) for the past 150 million years are in general agreement with the results from this model. **(B)** Radiative forcing for CO_2 calculated from (23) and corrected for changing luminosity (24) after adjusting for an assumed 30% planetary albedo. Deep-sea oxygen isotope data over the past 100 Ma (13, 14) have been scaled to global temperature variations according to (7). **(C)** Oxygen isotope-based low-latitude paleotemperatures from (5). **(D)** Glaciological data for continental-scale ice sheets modified from (7, 8) and based on many sources. The duration of the late Neoproterozoic glaciation is a subject of considerable debate.

Crowley & Berner (2002) *Science*, Vol. 292:870.

However, even with well-preserved foraminifera, Cretaceous warmth may have commenced *after* large (inferred) CO_2 emission by seafloor spreading…

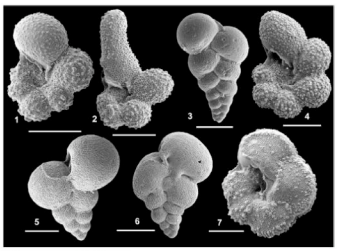

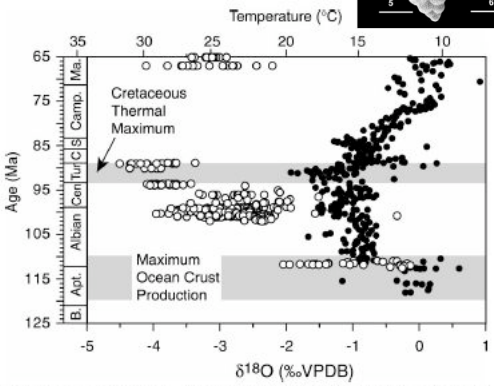

Figure 3. Comparison of Cretaceous $\delta^{18}O$-temperature records indicates 20–40 m.y. mismatch between peak Cretaceous-Cenozoic global warmth (Cretaceous thermal maximum) and peak Cretaceous-Cenozoic tectonic CO_2 production inferred from ocean-crust cycling (Larson, 1991). Glassy planktic foraminifera (open symbols) from low-latitude western tropical Atlantic (plus Maastrichtian data from Tanzania and Gulf Coast) vs. bulk carbonate (solid symbols) from high-latitude Southern Indian Ocean (Clarke and Jenkyns, 1999; Erbacher et al., 2001; Wilson and Norris, 2001; Pearson et al., 2001; Norris et al., 2002). All temperatures calculated in same way as conservative temperatures in Figure 2 and would be 3–6 °C higher if modern latitudinal trends in δw (global mean Cretaceous seawater) were applied (see text).

Wilson et al. *Geology* (2002)

Other Evidence for Weak CO_2 - Climate Connection during Phanerozoic

$\varepsilon_p \sim pCO_2$

$\varepsilon_p \sim \varepsilon_{toc} = \delta^{13}C_{CaCO3} - \delta^{13}C_{org}$

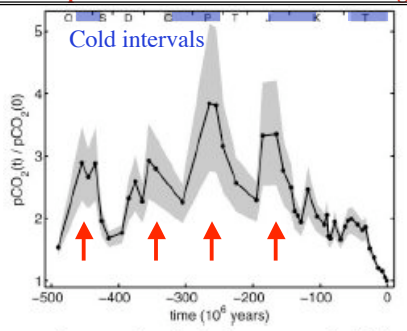

Fig. 4. Fluctuations of pCO_2 for the last 500 My, normalized by the estimate of pCO_2 obtained from the most recent value of ζ. The solid line is obtained from Eq. 12 by using $\kappa_0 = 36‰$. The lower and upper limits of the gray area surrounding the pCO_2 curve result from $\kappa_0 = 38$ and 35‰, respectively. The gray bars at the top correspond to periods when Earth's climate was relatively cool; the white spaces between them correspond to warm modes (18).

Rothman (2002) *PNAS*

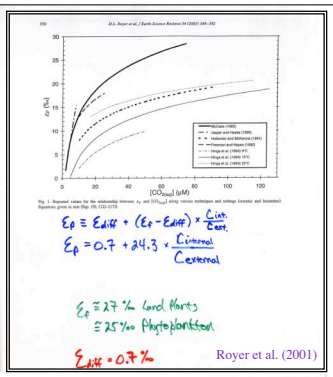

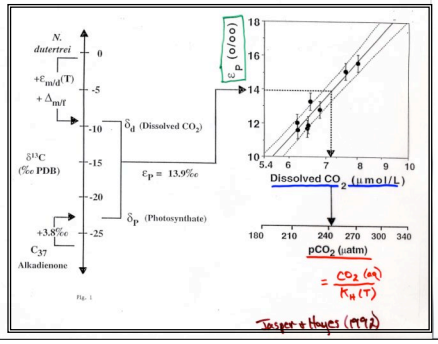

But different CO_2 proxies lead to different results….

$\varepsilon_{toc}=\delta^{13}C_{CaCO3}-\delta^{13}C_{org}$

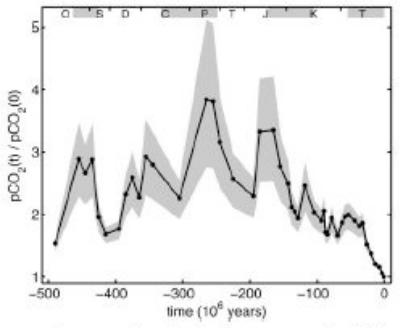

Fig. 4. Fluctuations of pCO_2 for the last 500 My, normalized by the estimate of pCO_2 obtained from the most recent value of ξ. The solid line is obtained from Eq. 12 by using $\varepsilon_D = 36‰$. The lower and upper limits of the gray area surrounding the pCO_2 curve result from $\varepsilon_D = 38$ and 35‰, respectively. The gray bars at the top correspond to periods when Earth's climate was relatively cool; the white spaces between them correspond to warm modes (18).

Rothman (2002)

Soil carbonate δ ^{13}C & geochemical model

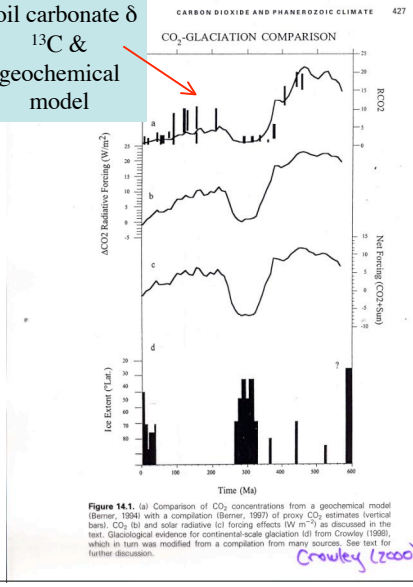

Figure 14.1. (a) Comparison of CO_2 concentrations from a geochemical model (Berner, 1994) with a compilation (Berner, 1997) of proxy CO_2 estimates (vertical bars). CO_2 (b) and solar radiative (c) forcing effects (W m^{-2}) as discussed in the text. Glaciological evidence for continental-scale glaciation (d) from Crowley (1998), which in turn was modified from a compilation from many sources. See text for further discussion.

Crowley (2000)

Other evidence for Low CO_2 During Known Warm Periods

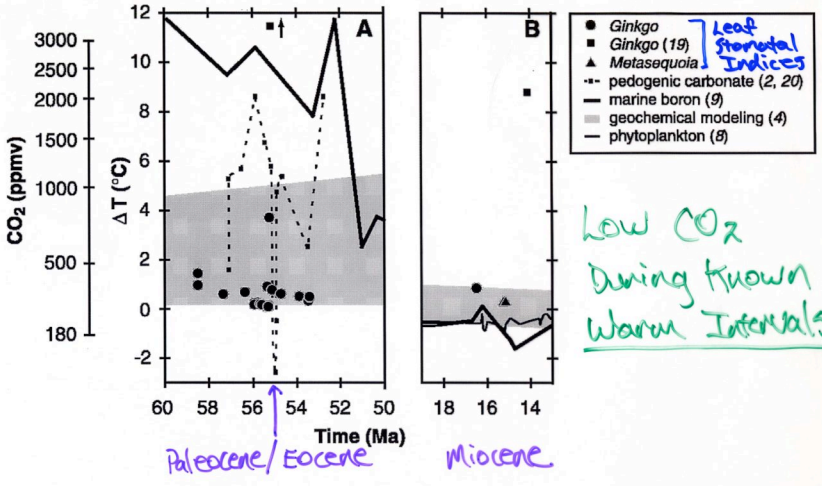

Low CO_2 during known warm intervals

Royer, et al. (2001) Science, Vol. 292, p. 2310

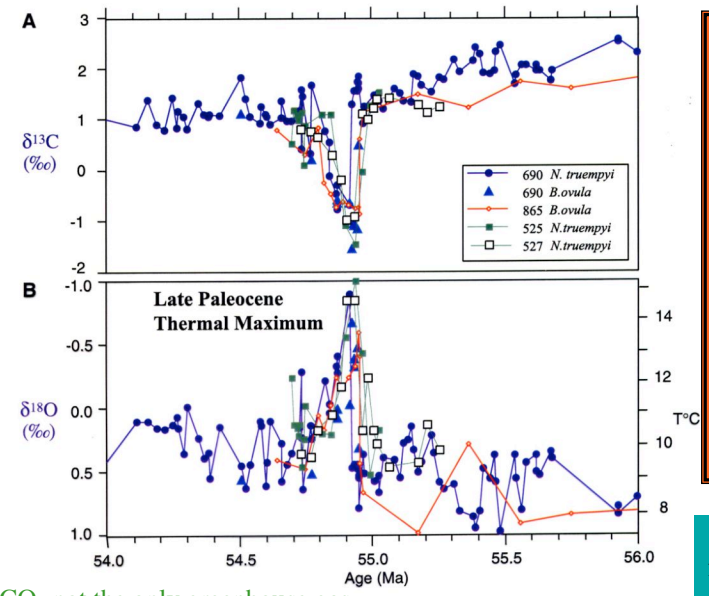

Gas Hydrate Release of Methane (2600 Gt) caused Late Paleocene Thermal Maximum

Benthic foraminifera from Atlantic & Pacific

- CO_2 not the only greenhouse gas we need to consider when evaluating warm episodes.

Zachos et al. (2001)

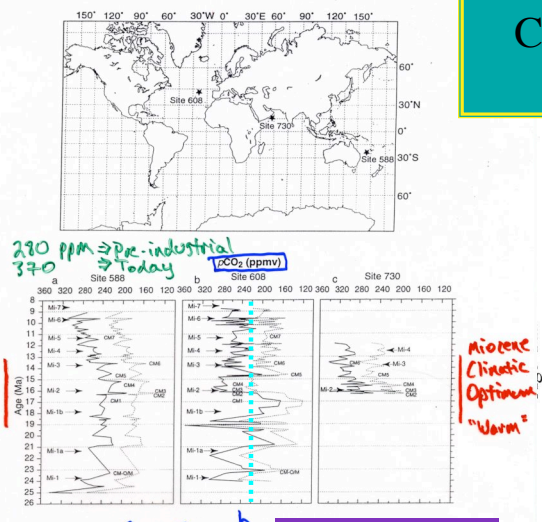

Pre-Industrial CO_2 levels!

Further Evidence for Low CO_2 During Miocene Warm Period

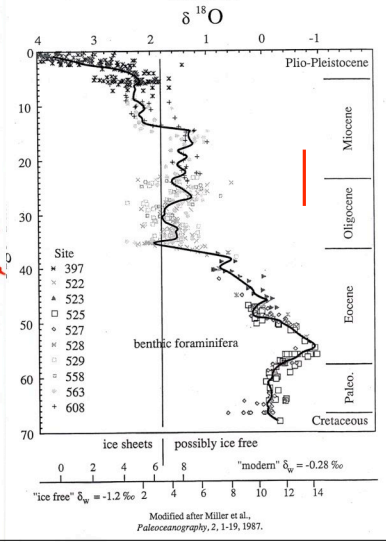

Carbon Isotopic Fractionation Indicates pCO_2

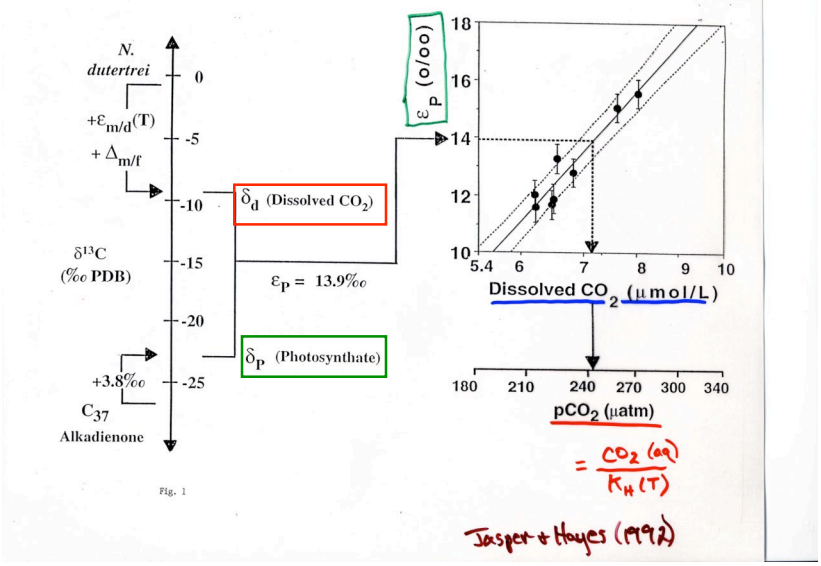

Substantial evidence exists for a strong link between CO_2 & climate on a variety of timescales…. With some notable exceptions!

Additional paleoclimate reconstructions & numerical model simulations are necessary. But the biggest (non-controlled) experiment ever attempted is now underway…

External Influences on Climate

The Sun & Planets to Scale

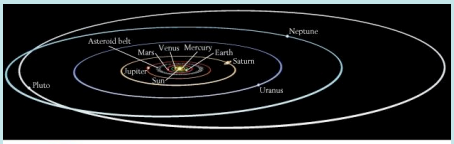

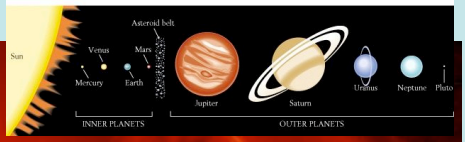

NASA-JPL

The Asteroid Belt

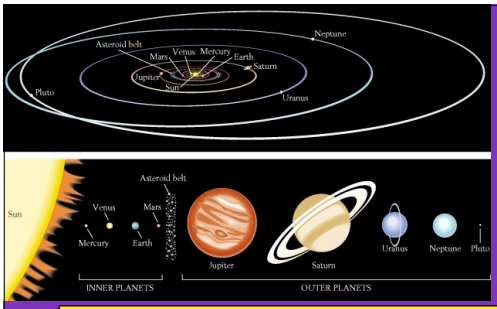

- A relic of the accretion process. A failed planet.
- Gravitational influence of Jupiter accelerates material in that location to high velocity.
- High-velocity collisions between chunks of rock shatter them.
- The sizes of the largest asteroids are decreasing with time.

Total mass (Earth = 1)	0.001
Number of objects > 1 km	~100,000
Number of objects > 250 km	~12
Distance from Sun	2-4 AU
Width of asteroid belt (million km)	180

Earth Accretion Rate Through Time

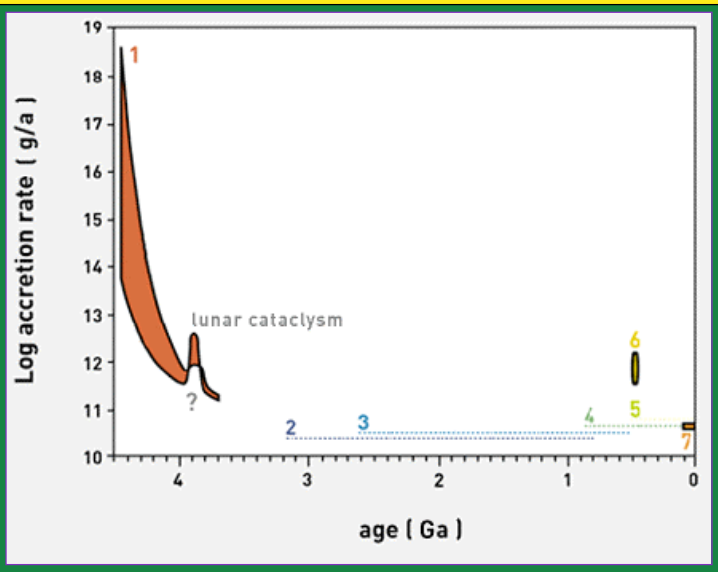

Schmitz et al.. (1997) *Science*, Vol. 278: 88-90, and references therein.
http://www.whoi.edu/science/MCG/pge/project4.html

Accretion continues…

Chicxulub Crater, Gulf of Mexico
- 200 km crater
- 10-km impactor
- 65 Myr BP
- Extinction of 75% of all species!

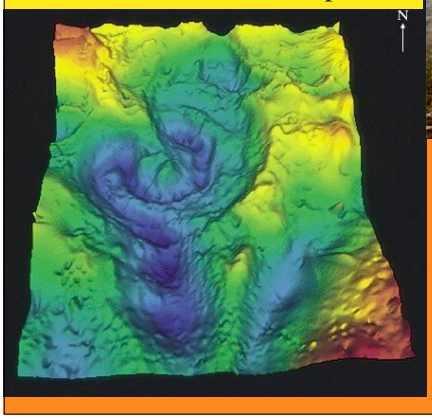

Meteor (Barringer) Crater, Arizona
- 1 km diam. Crater
- 40-m diam Fe-meteorite
- 50 kyr BP
- 300,000 Mton
- 15 km/s

http://www.gi.alaska.edu/remsense/features/impactcrater/imagexplain.htm

Interplanetary Dust Accumulation

http://presolar.wustl.edu/work/idp.html

40±20 x10^4 metric tons/ yr (40 x10^{10} g) interplanetary dust accretes every yr!

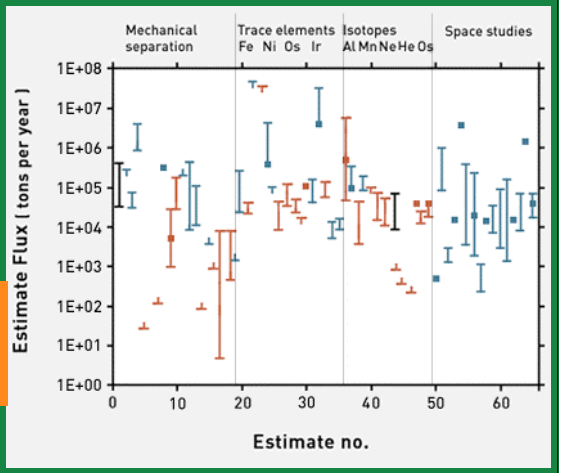

http://www.whoi.edu/science/MCG/pge/project4.html

Size - Frequency Distribution of Impacts

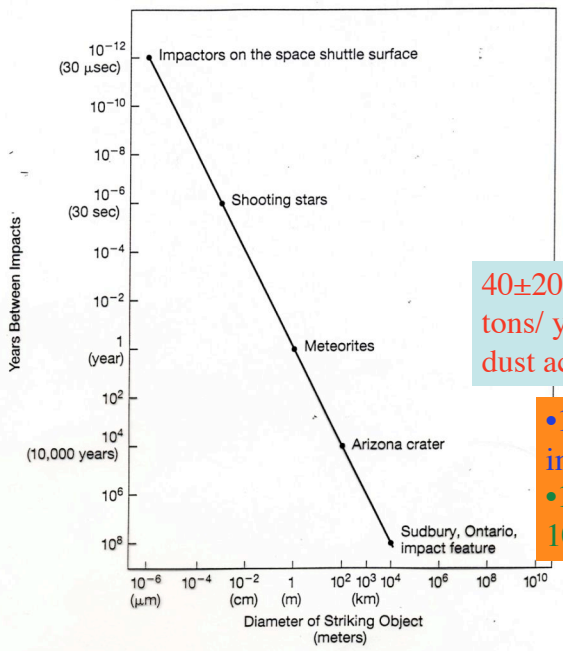

40±20 x 10^4 metric tons/ yr interplanetary dust accretes every yr!

- 100 m object impacts every 10 kyr
- 10 km object every 100 Myr

Kump et al. (1999)

Chicxulub Crater Gulf of Mexico

- 200 km crater
- 10-km impactor
- 65 Myr BP
- Extinction of 75% of all species!

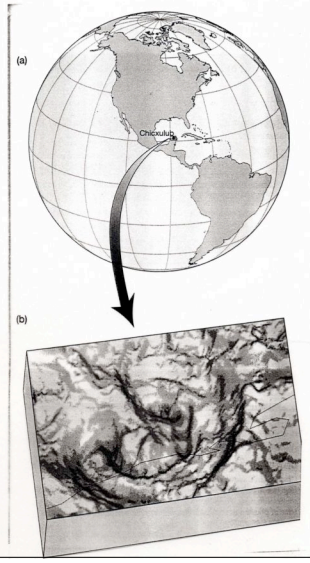

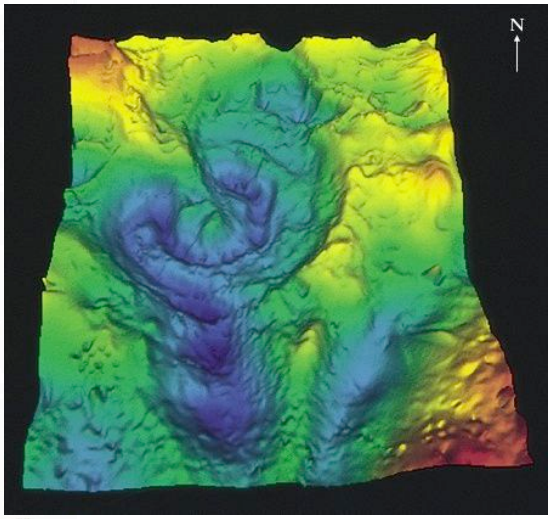

Evidence for Meteorite Impact @ K-T Boundary

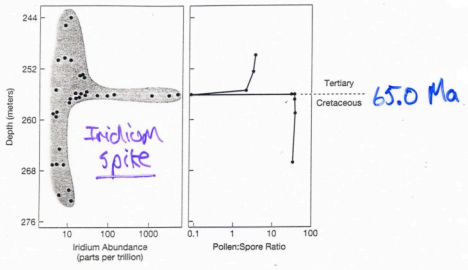

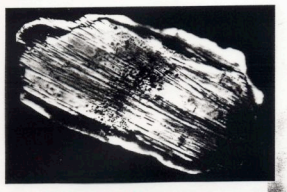

↑ Pressure
Shocked Quartz

↑ Temperature
Microspherules

(b)

Phanerozoic History of Extinctions

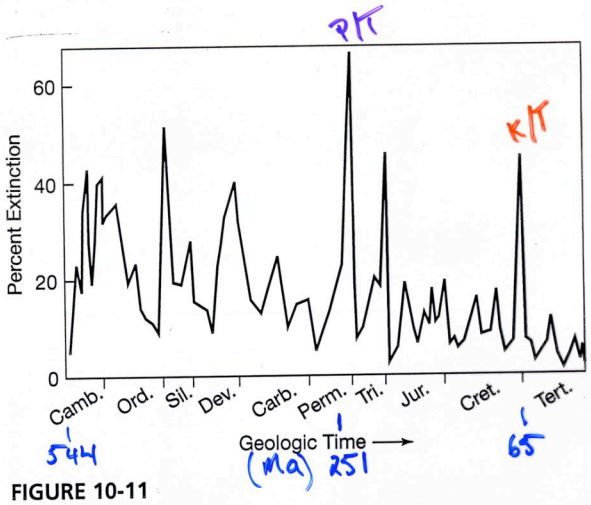

FIGURE 10-11

The fossil record of extinction rate, shown as the percentage of existing genera that went extinct in a particular interval (*stage*) of geologic time. (After Sepkoski, J.J. Jr., *Geotimes*, March, 1994, 15–17.)

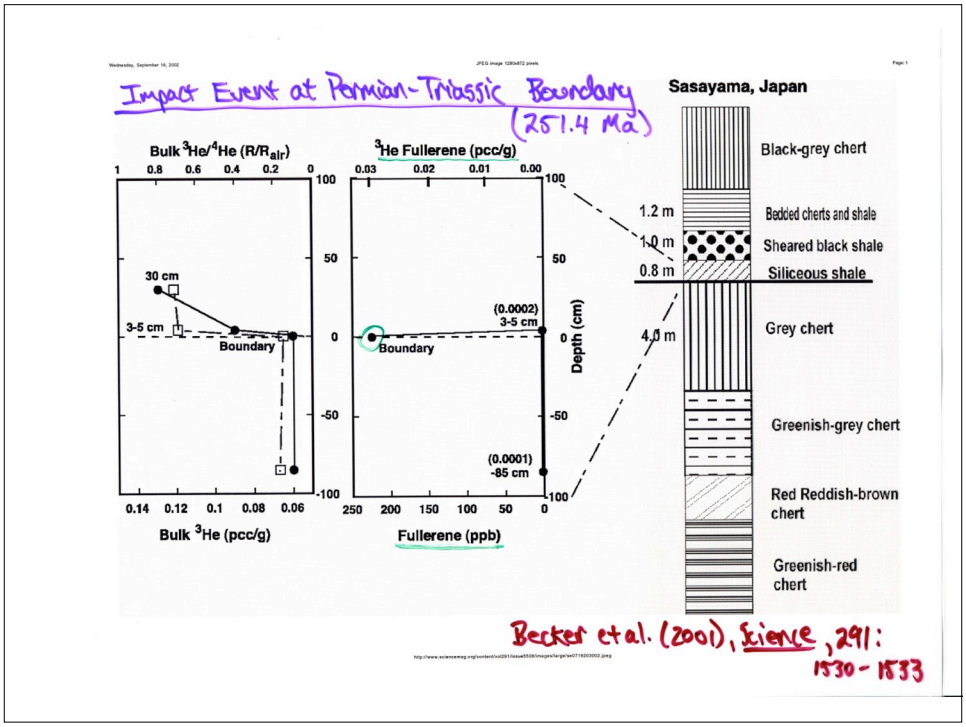

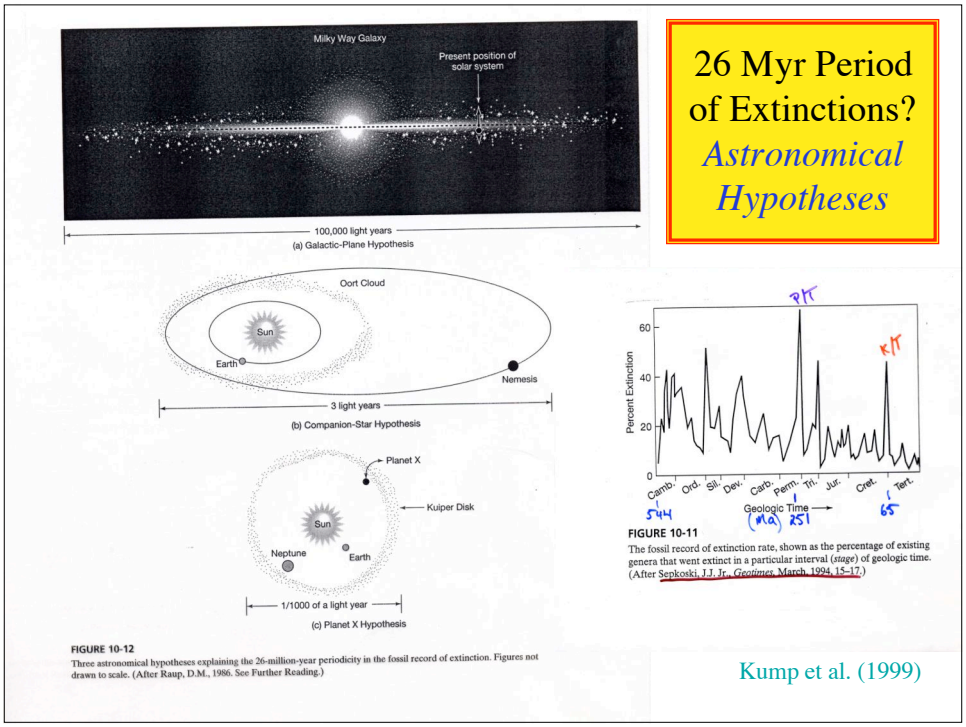

26 Myr Period of Extinctions?
Astronomical Hypotheses

Kump et al. (1999)

Cosmic Ray Forcing of Climate?

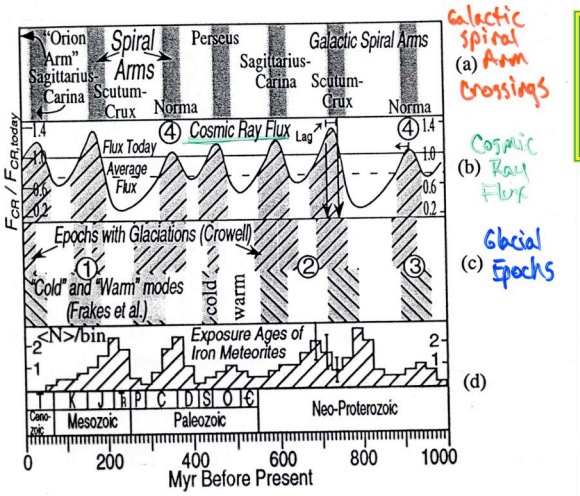

Galactic spiral Arm Crossings

Cosmic Ray Flux

Glacial Epochs

Shaviv (2002), Phys. Rev. Lett., v.89(5): 051102-1-4

$\frac{F_{CR}}{F_{CR,today}}$: 25% - 135%

$\frac{T}{T_{today}}$: +10 -5 K

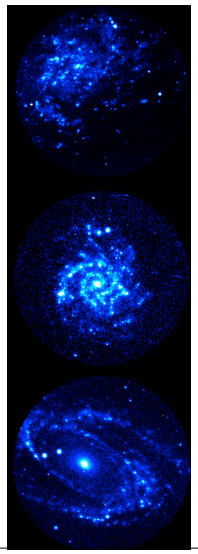

http://antwrp.gsfc.nasa.gov/apod/ap960409.html

Cosmic Ray Influence on Climate?

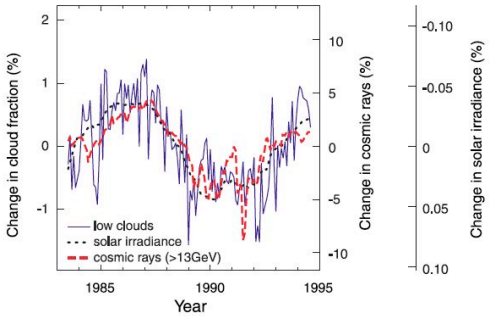

Fig. 1. Variation of low-altitude cloud cover, cosmic rays, and total solar irradiance between 1984 and 1994. The cosmic ray intensity is from Huancayo observatory, Hawaii. [Adapted from (*4*)]

Carslaw et al. (2002) *Science* Vol. 298: 1732-1737.

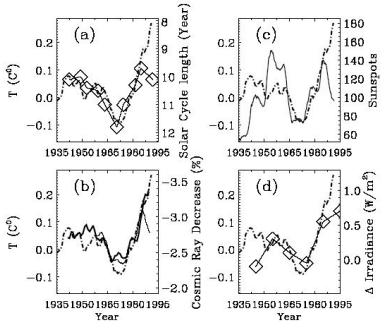

FIG. 3. 11 year average of northern hemispheric marine and land temperatures (dash-dotted line) compared with (a) unfiltered solar cycle length; (b) 11 year average of cosmic ray flux (from ion chambers 1937–1994, normalized to 1965), thick solid line; the thin solid line is cosmic ray flux from Climax, Colorado neutron monitor (arbitrarily scale); (c) 11 year average of relative sunspot number; (d) decade variation in reconstructed solar irradiance (zero level corresponds to 1367 W/m^2, adapted from Lean *et al.* [6]). Note the 11 year average has removed the solar cycle in (b) and (c).

Svensmark (1998) *Phys. Rev. Lett.* Vol. 81(22): 5027-5030.

Correlation Is Not Causation

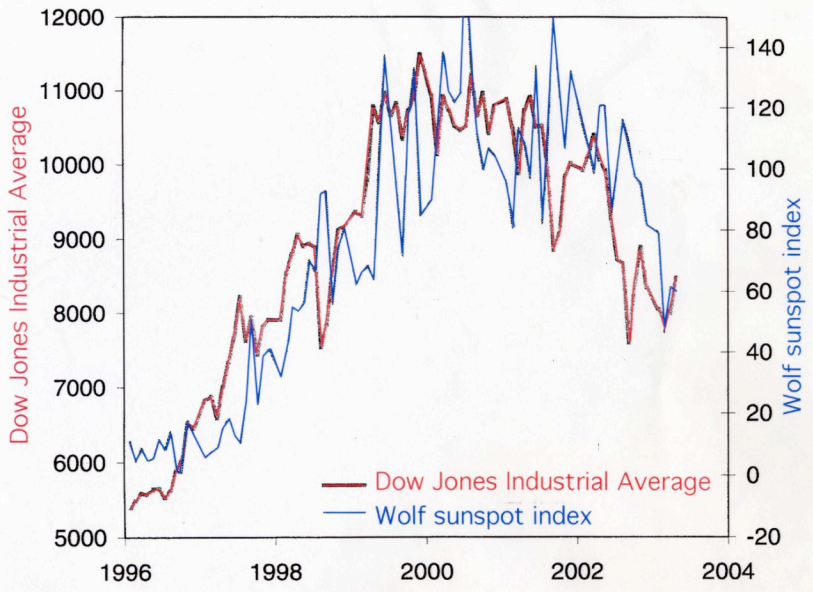

Earth's Climate
Part 4

Pleistocene Glaciations

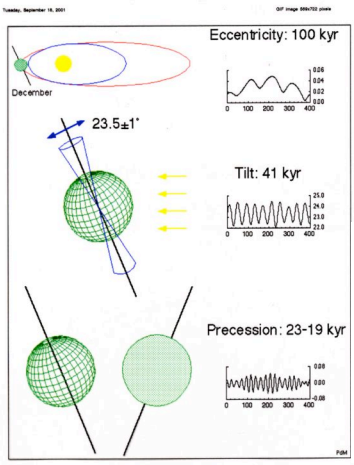

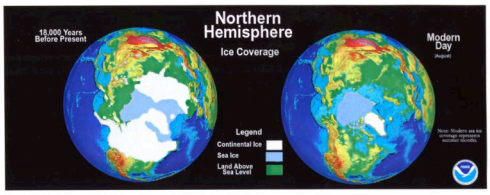

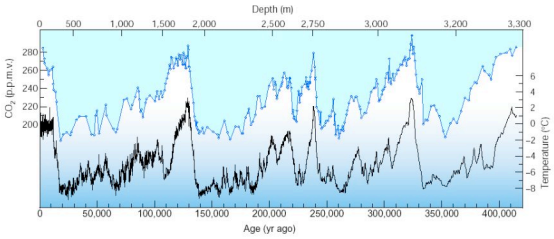

Earth's Orbital Geometry:

The Milankovitch Hypothesis & the Pacing of Pleistocene Ice Ages

Milankovitch Hypothesis: Historical Perspective

What: Astronomical theory of Pleistocene ice ages.

How: Varying orbital geometry influences climate by changing seasonal & latitudinal distribution of solar radiation incident at top of atmosphere (insolation).

Milestones: Hypothesis

- Croll (1864, 1875): Proposed that variations in seasonal influx of energy--the cumulative affect of eccentricity, obliquity & precession--could trigger large climate response.
- Milankovitch (1920, 1941): Combined laws of radiation with planetary mechanics to derive insolation curves as function of time (600 kyr) and latitude. Concluded summer insolation at high N. lat. (65°N) critical to growth/decay of ice sheets. "The Milankovitch Hypothesis".

James Croll, 1896

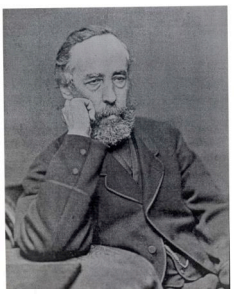

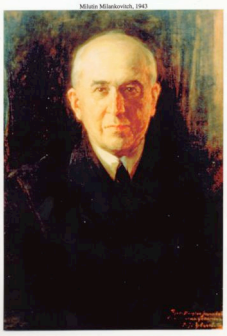

Eccentricity, Obliquity (tilt), Precession

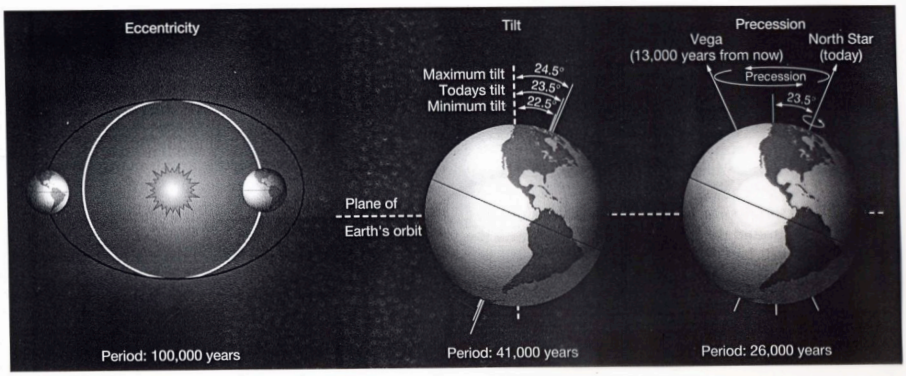

FIGURE 11-5

Aspects of Earth's orbit around the Sun that have implications for climate change. (a) The elliptical nature of the orbit (eccentricity) changes on 100,000-year time scales. (b) The tilt of the spin axis with respect to the plane of Earth's orbit around the Sun (obliquity) changes on a 41,000-year time scale. (c) The orientation of the spin axis in space wobbles (precesses) with periodicities of 19,000 and 23,000 years. (From J.P. Davidson, W.E. Reed, and P.M. Davis: *Exploring Earth: An Introduction to Physical Geology*, 1997. Reprinted by permission of Prentice Hall, Upper Saddle River, N.J.)

Kump et al. (1999)

Eccentricity of Present Earth Orbit Around Sun (to Scale)

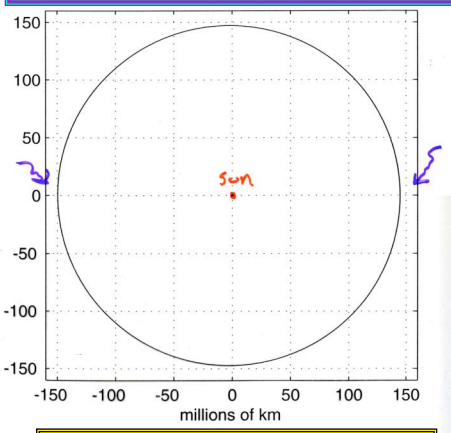

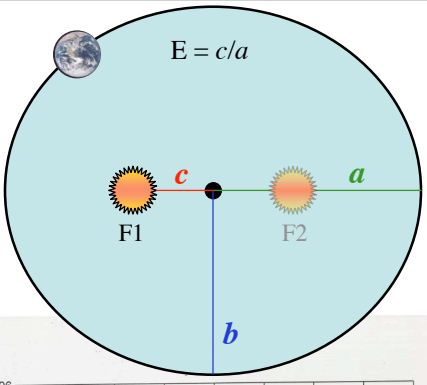

Present eccentricity = 0.017
Range: 0 - 0.06
100 & 400 kyr periods

Muller & MacDonald (2000)

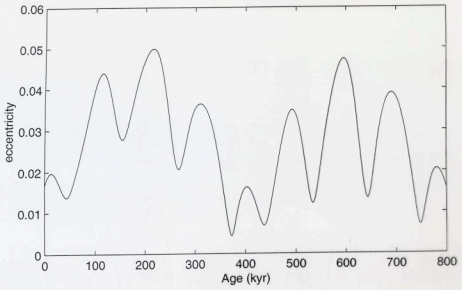

Fig. 2.6. The eccentricity of the Earth's orbit.

Obliquity

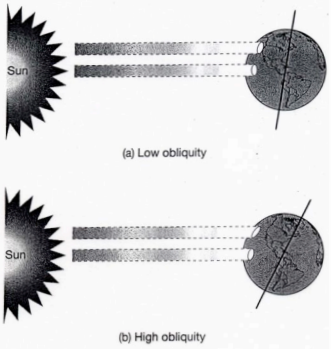

FIGURE 11-7
(a) At low obliquity, Earth has less contrast in insolation between the seasons. (b) At high obliquity, the seasonal contrast is greater.

Kump et al. (1999)

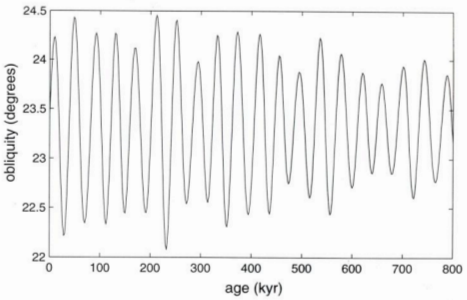

Fig. 2.12. Obliquity.

Muller & MacDonald (2000)

2 Types of Precession

I. Precession of Spin Axis

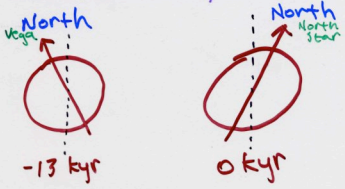

Side view

26 kyr Period Top view

II. Precession of Perihelion

→ opposite direction from spin axis precession

∴ 23-19 kyr Period

Today: Dec/Jan June/July

Precession

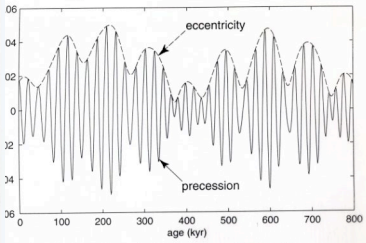

Fig. 2.10. Precession parameter p and eccentricity.

$p = e \sin \omega$

ω ↑∠ between spring Equinox Solstice + perihelion

Muller & MacDonald (2000)

Wednesday, September 19, 2001 Large Paleo Slide Images Page: 1

Precession of Earth's orbit adapted from Pisias and Imbrie [1986/1987]

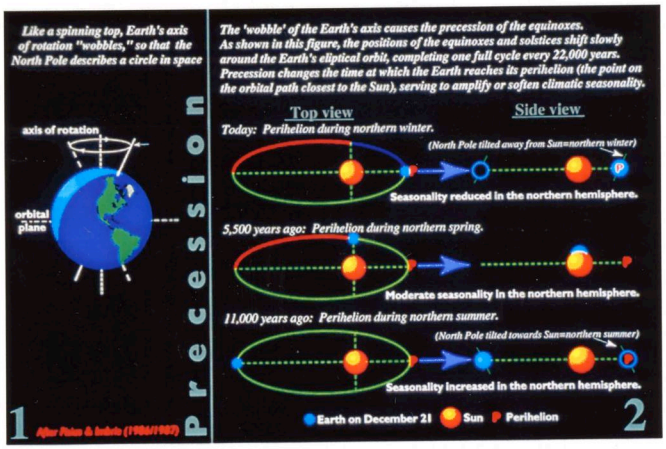

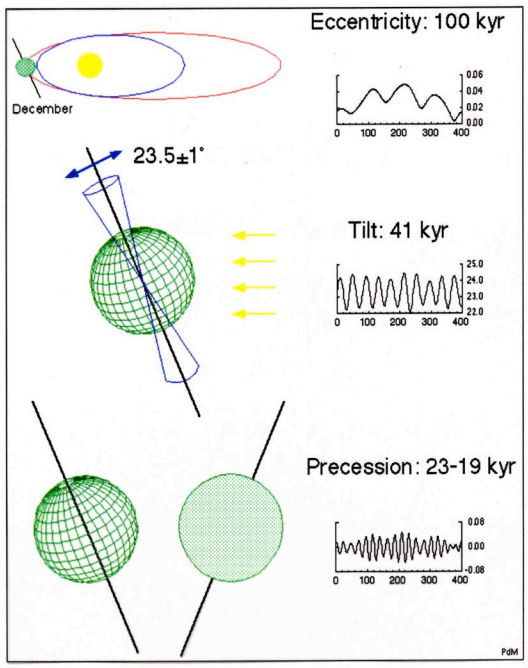

Periodic changes in orbital geometry modulate solar radiation receipts (insolation)

Summer (June 21) Insolation at 65°N

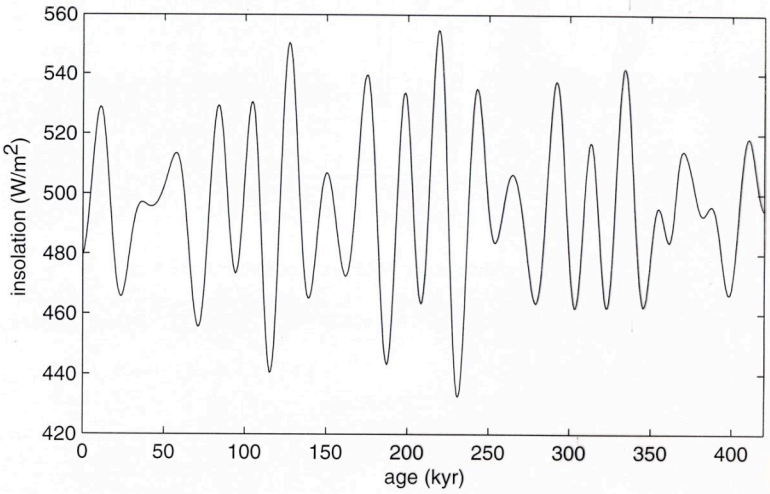

Fig. 4.38. Insolation, July 65N. Note similarity to Fig. 4.37.

Muller & MacDonald (2000)

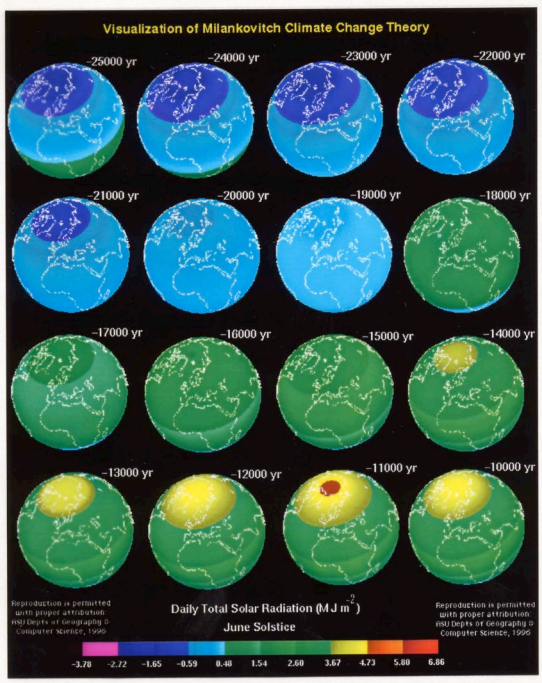

Increasing Northern Hemisphere insolation caused the end of the last ice age?

Milankovitch Hypothesis: Milestones & Support

- Kullenberg (1947): Invented deep-sea piston coring.
  →Recovery of long, continuous climate records possible.
- Emiliani (1955): Pioneered use $^{18}O/^{16}O$ ratio of fossil foraminifera in sediment cores as climate (temp.) proxy.
- Olausson (1965); Shackleton (1967): Interpret foram $\delta^{18}O$ changes as whole-ocean isotopic shifts caused by ice sheet growth/decay.
- 1960's: Recognition of magnetic stripes on ocean floor (geomagnetic field reversals) as global stratigraphic markers.
- Johnson (1982); Shackleton et al (1990): Use astronomically-driven insolation variations (E, T, P) to derive timescales for deep-sea cores.
  →Accurately predict age of Brunhes-Matuyama (B/M) magnetic reversal, 780-790 kyr BP. (K/Ar dates for B/M incorrectly placed it at 730 kyr BP.)
- Baksi et al (1992): $^{40}Ar/^{39}Ar$ date for B/M = 783 kyr BP.
- Raymo (1997): Multiple $\delta^{18}O$ records on 'simple' timescale supports link between N. Hemisphere summer insolation and glacial terminations.

→Strong support for astronomical influence on climate. (The magnitude of which remains debated…)

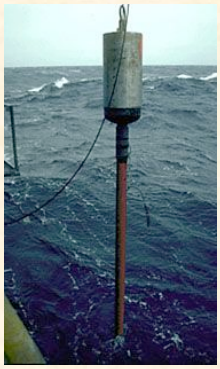

T-dependent Isotopic Fractionation

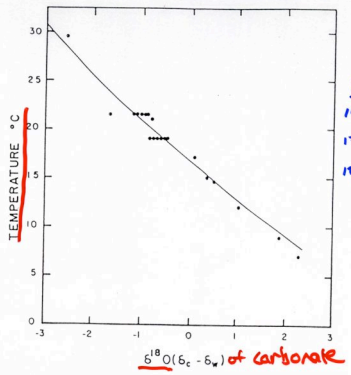

Natural Abundances
^{16}O = 99.756%
^{17}O = 0.039
^{18}O = 0.205

$CaC^{16}O_3 + H_2{}^{18}O \leftrightarrow CaC^{16}O_2{}^{18}O + H_2{}^{16}O$

$T = 16.9 - 4.2(\delta^{18}O_c - \delta^{18}O_w)$

$\delta^{18}O_w = f(\text{Salinity, ice volume})$

$\delta^{18}O = \left[\frac{(^{18}O/^{16}O)_{sample}}{(^{18}O/^{16}O)_{standard}} - 1\right] \times 1000‰$

Epstein et al. (1953)

A Temperature-Dependent Isotopic Fractionation of ^{18}O from ^{16}O Occurs During Calcification

Photo of *Helenina anderseni*

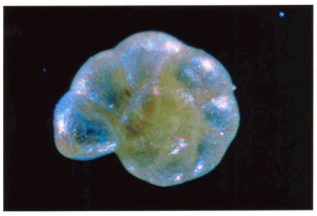

Foraminifera

$\delta^{18}O$ of Seawater varies w/ Salinity

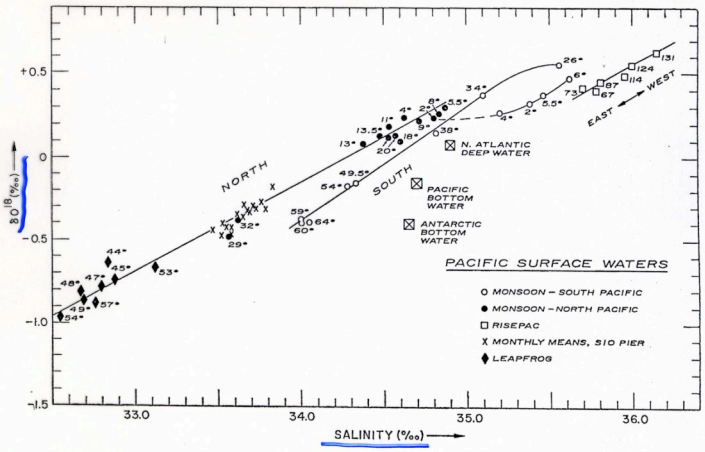

FIGURE 10. — *Oxygen 18-salinity relationships in surface and deep Pacific Ocean samples. Latitudes are shown for Monsoon and Leapfrog samples: the figures on the Risepac expedition points are station numbers shown in figure 6.*

H. Craig and L. I. Gordon (1965)

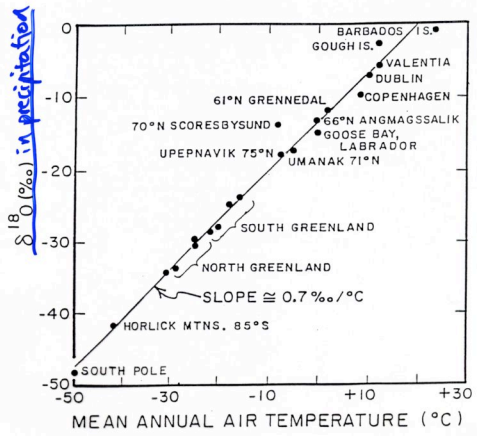

Dansgaard (1964)

- $\delta^{18}O$ of precipitation varies with latitude & altitude.
- Water derived from melting snow & ice is highy depleted in ^{18}O.
- Airmass trajectory influences $\delta^{18}O$ of precipitation

$H_2{}^{18}O$ has 1% lower vapor P

∴ Cold Air (High latitude +/or Altitude) has low $\delta^{18}O$

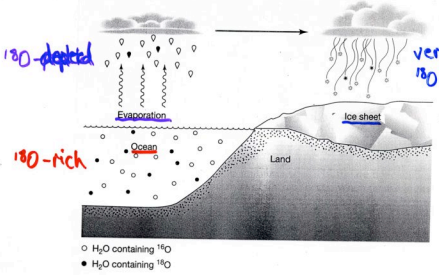

Influence of Ice Volume on Ocean $\delta^{18}O$

1.3‰ Decrease of Ocean $\delta^{18}O$ from Melting Glaciers

120 M Sea Level Depression @ LGM

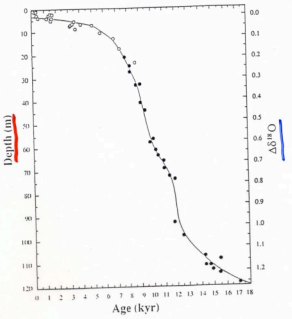

FIG. 2 Barbados sea level curve based on radiocarbon-dated *A. palmata* (filled circles) compared with *A. palmata* age-depth data[4] (open circles) for four other Caribbean island locations. All radiocarbon ages in this figure are corrected for local seawater $\Delta^{14}C$ by subtracting 400 yr from the measured radiocarbon ages[4] but they are not corrected for secular changes in atmospheric ^{14}C levels[15]. The Barbados data are corrected for the estimated mean uplift of 34 cm kyr^{-1}. The right-hand axis of the Barbados sea level curve (solid line) is scaled to the estimated $\delta^{18}O$ change of mean ocean water using the calibration in ref. 5.

Fairbanks (1989), Nature, 342: 637-642

Global Variation of $\delta^{18}O$ in Precipitation

Numerical mean ∂ values of annual precipitation, covering periods of 2 to 10 years, and approximate iso-∂-lines; ∂ values are relative per mille deviations of O^{18}/O^{16} ratios from Standard Mean Ocean Water [1]. The influence of the present Gulf Stream is seen very clearly in the course of the isoline for ∂ = -10 per mille. The dashed line indicates the maximum extension of continental ice and permanent pack ice during the last glacial maximum according to Flint [2].

[1] Craig, H. (1961) *Science* **133**, 1833.
[2] Flint, R.F. (1957) Glacial and Pleistocene Geology. New York: Wiley, plate 3.

Adapted from: Dansgaard, W. (1969) Glacier Oxygen-18 Content and Pleistocene Ocean Temperatures, *Science* **166n**, 3904, pp. 499-502.

Note: All values should be *negative*.

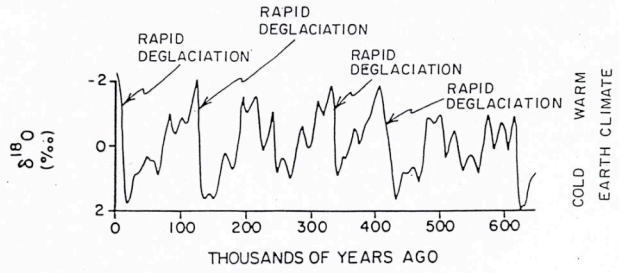

Figure 5. The ^{18}O-^{16}O record for benthic foraminifera from deep sea sediments. The oxygen isotope results are given as percent difference in the ^{18}O to ^{16}O ratio from that in an international reference standard. The more positive the $\delta^{18}O$ value the larger the ^{18}O content of sea water. As the growth of ice caps enriches sea water in ^{18}O, these high values correspond to times of large continental ice cover. The time scale was obtained from radioisotope measurements on the deep sea sediments. Although not a regular progression, the times of large ice cover follow one another at roughly 100,000 year intervals. Note also the rapidity with which the largest of these ice masses disappeared!

Magnetic Stripes

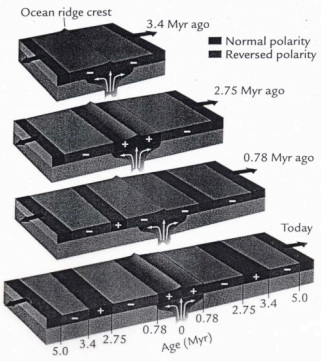

FIGURE 5-8 **Magnetization of ocean crust** Successive bands of ocean crust form as molten lava erupts at the seafloor, cools, and solidifies. The new crust is magnetized in the normal or reversed polarity prevailing at the time. As the plates move apart, equal amounts of magnetized crust are carried away from the ridge axis in both directions and can be used to date the seafloor. (Modified from F. Press and R. Siever, *Understanding Earth*, 2nd ed., © 1998 by W. H. Freeman and Company.)

Magnetic Stratigraphy

① $^{40}Ar/^{39}Ar$ - date lava flows

② Apply dates to downcore reversals

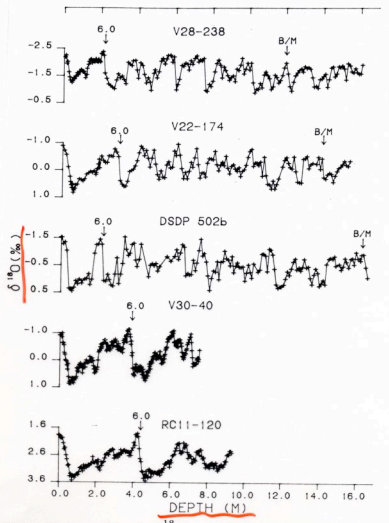

Figure 4 Variations in $\delta^{18}O$ as a function of depth in five deep-sea cores. Two important stratigraphic levels are labeled as follows : 6.0 for the boundary between isotope stages 5 and 6; and B/M for the magnetic reversal at the Brunhes-Matuyama boundary. See Table 1.

Imbrie et al. (1984)

Simple Timescale

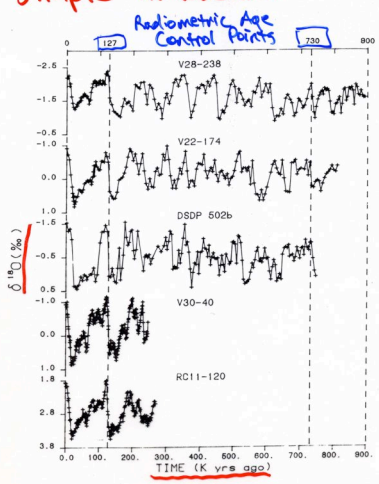

Figure 5 Variations in $\delta^{18}O$ as a function of estimated time in five deep-sea cores. The time scale is derived by linear interpolation between (and extrapolation beyond) control points at 127 KY, 730 KY BP. For details, see text and Table 5.

Imbrie et al. (1984)

Filter $\delta^{18}O$ Record at Obliquity & Precession Frequencies

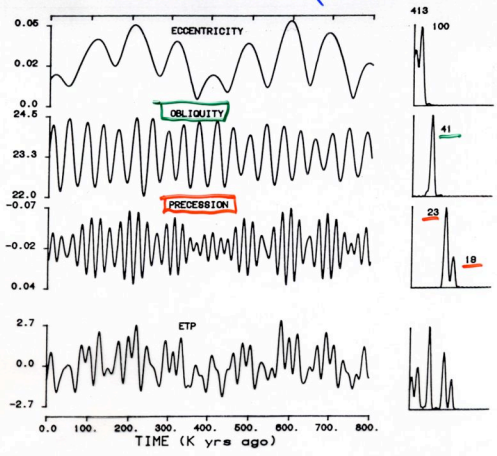

Figure 2 Variations in eccentricity, obliquity, and the precession index (Δ e sin ω) over the past 800 000 years. Left: The three upper time series are from the work of Berger (1). These have been normalized and added to form the curve labeled ETP. The scale for obliquity is in degrees; for ETP, in standard deviation units. Right: Variance spectra calculated from these time series, with the dominant periods (KY) of conspicuous peaks indicated.

Imbrie et al. (1984)

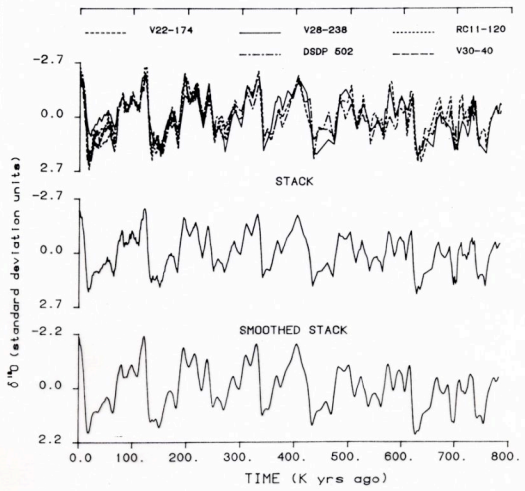

Figure 8 $\delta^{18}O$ variations in five deep-sea cores normalized and plotted on the SPECMAP time scale. In the top panel, data from each core has been normalized to zero mean and unit standard deviation. After interpolation at intervals of 1 KY, these curves have been averaged (middle panel), and smoothed with a 9-point Gaussian filter (bottom panel).

Imbrie et al. (1984)

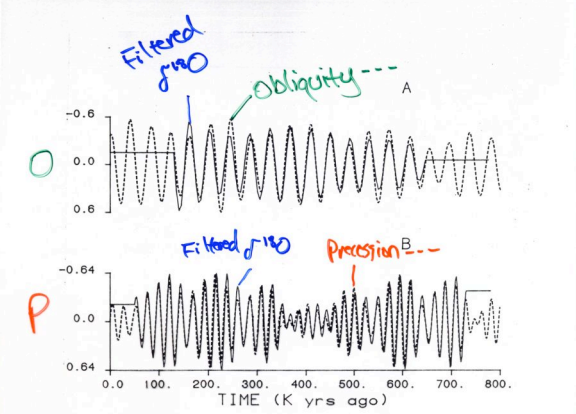

Figure 9 Variations in obliquity, precession, and the corresponding frequency components of $\delta^{18}O$ over the past 800 KY. Dashed lines are phase-shifted versions of obliquity (A) and precession (B) curves. Solid lines are filtered versions of the stacked $\delta^{18}O$ record plotted on the SPECMAP time scale. The filters used were centered on periods of 41 KY (A) and 22 KY (B). All curves have been transformed to have zero means with arbitrary scales.

High coherence (i.e., amplitude correlation) lends support to astronomical forcing of climate.

Imbrie et al. (1984)

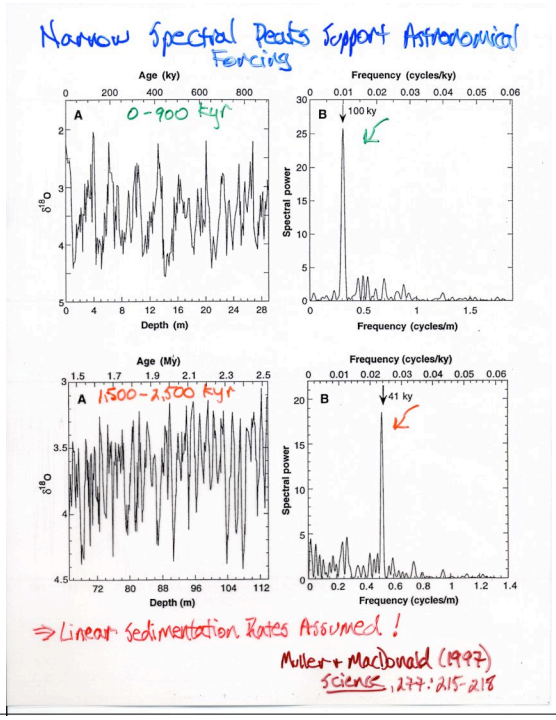

1. Why is climate response in 100-kyr band so strong?

Observation: High correlation of $\delta^{18}O$ cycles with astronomically-driven radiation cycles at E, T & P frequencies suggests causal link in all 3 bands.

Problem: Amplitude of insolation change (~0.2%) is ~10x smaller than in T,P bands.

Possible Solution: E modulates climatic effect of P. High E favors NH glaciation when P causes NH summer to occur at maximum Earth-Sun distance (i.e., Imbrie et al, 1993).

2. Why do glacial cycles switch from 41-kyr to 100-kyr period ~700 kyr BP?

Possible solution: L/T cooling trend, perhaps from tectonically-driven decrease in atmospheric CO_2, facilitates NH ice sheet growth beyond a critical threshold during insolation minima. These large ice sheets drive climate through feedbacks internal to the climate system (geo-, cryo-, atmo-, hydro-sphere).

3. Why do full glacial Terminations, and ensuing interglacial periods, occur ~430 and ~15 kyr BP when E is very low?

-Possible solution: 100-kyr cycle of orbital inclination (Muller and MacDonald, 1995).

-Caveat: no obvious mechanism linking climate to inclination.

Milankovitch Hypothesis Challenges:

100-kyr Cycle Problems

Eccentricity Modulates Precession

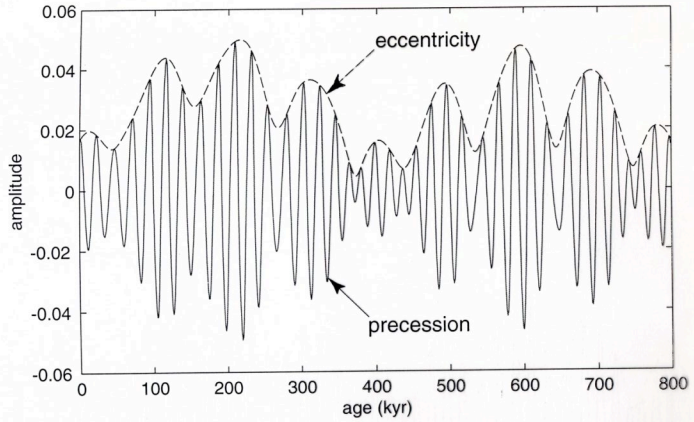

Fig. 2.10. Precession parameter p and eccentricity.

$p = e \sin \omega$

↑ ∠ between spring Equinox ~~Solstice~~ + perihelion

Muller & MacDonald (2000)

100-Kyr Cycle Problem-1

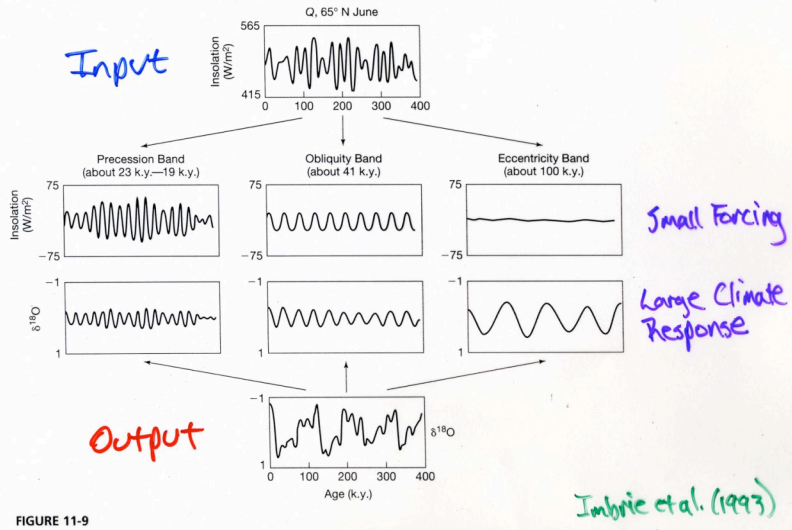

Imbrie et al. (1993)

FIGURE 11-9

Northern Hemisphere June insolation (Q, the climate forcing) and marine oxygen isotopic composition ($\delta^{18}O$, the climate response) and their dominant periodic components. (After Imbrie et al., *Paleoceanography* 7:701–738, 1992.)

100 kyr Climate Forcing from Orbital Inclination?

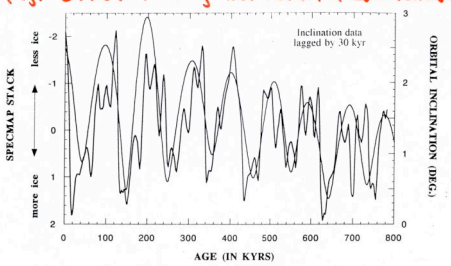

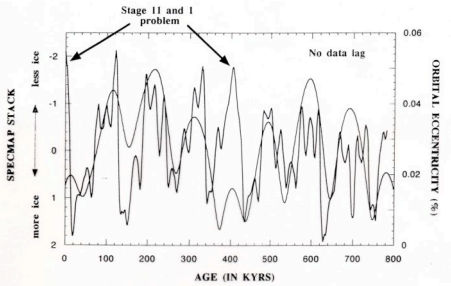

Muller + MacDonald (1995), Nature, v. 377: 107-108

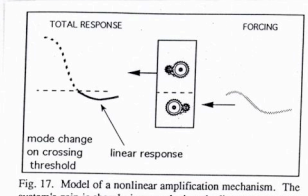

Fig. 17. Model of a nonlinear amplification mechanism. The system's gain is sharply increased when the linear response to an external forcing crosses a threshold.

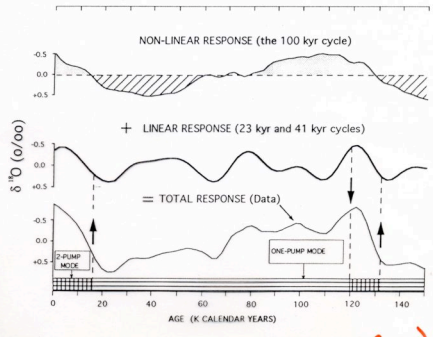

Imbrie et al. (1993)

The 100 kyr Cycle Problem - 2

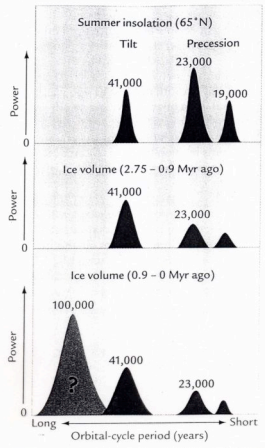

FIGURE 10-17 **Spectral analysis: insolation and ice volume** Summer insolation changes at 65°N occur only at the orbital rhythms of tilt (41,000 years) and precession (23,000 and 19,000 years) (top). Between 2.75 and 0.9 Myr ago, the $\delta^{18}O$ signal (northern hemisphere ice volume and deep-ocean temperature) contains the same rhythms as orbital insolation (middle). The large 100,000-year cycle evident in the $\delta^{18}O$ (ice volume) signal since 0.9 Myr ago is not present in the insolation signal (bottom).

Pleistocene Ice Age Cycles

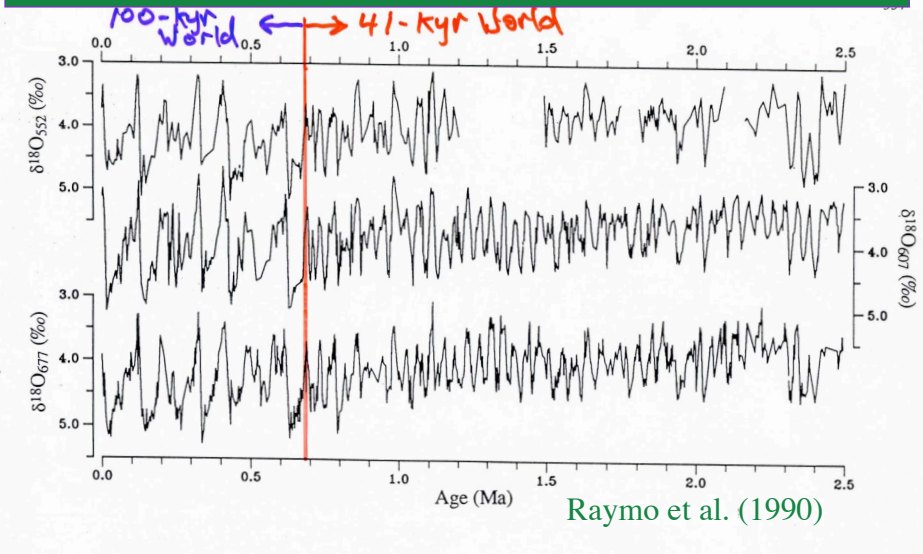

Raymo et al. (1990)

"100-kyr Ice"

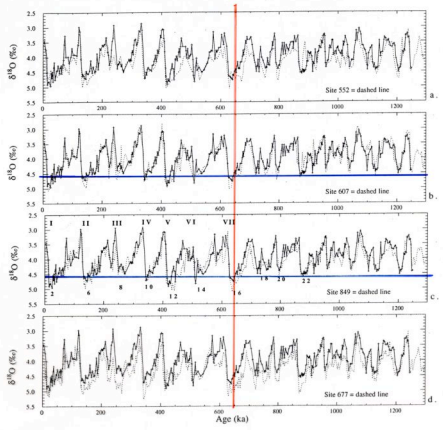

Figure 4. Oxygen isotope data (replicates averaged and species adjustments made) from sites 552, 607, 664, 849, and 677. The site 664 record is plotted on each panel to facilitate evaluation of correlations between these five sites. The horizontal lines in Figures 4b and 4c define the limits of "100K ice," the added ice volume which characterizes the Brunhes "100 ka world." In Figure 4c the major terminations of the late Pleistocene are labeled (I-VII), as are selected marine oxygen isotope stages.

Raymo et al. (1997)

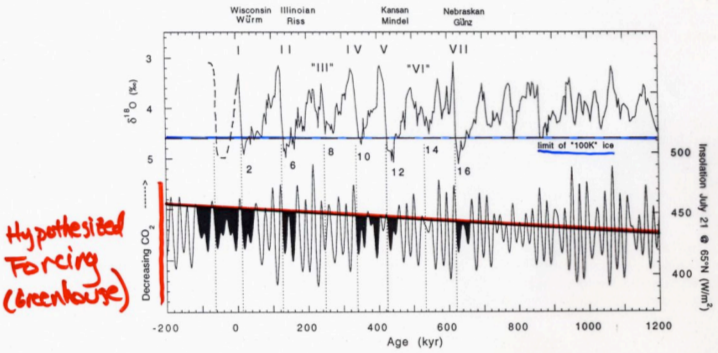

Hypothesized Forcing (Greenhouse)

■ = Sufficiently low insol. for 100k ice

Figure 5. Benthic $\delta^{18}O$ data from Pacific Site 849 plotted to the GSS97 timescale. Insolation received on July 21 at 65°N is shown on lower half of figure [after *Laskar et al.*, 1993]. This site is representative of the pattern of ice volume change over the last 800 kyr and can be compared with other records plotted in Figure 1. The horizontal dashed line on the $\delta^{18}O$ record indicates the level below which 100-kyr ice is observed. Terminations and selected isotope stages are labeled, as well as the historical names of the glacial stages. On the insolation record, the fiducial level below which 100-kyr ice can nucleate and be stable (shaded regions) is indicated by the slanted horizontal line. The vertical dashed lines indicate the midpoint of terminations using the GSS97 timescale.

Raymo (1997)

420,000 Years of Climate at Vostok, Antarctica

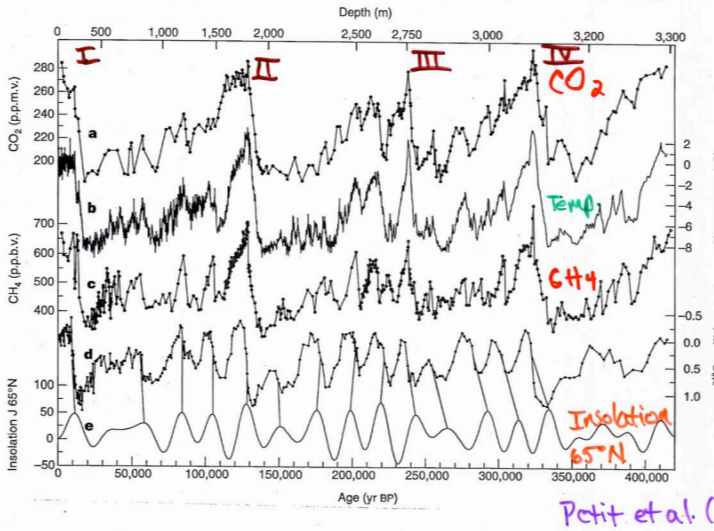

Petit et al. (1999)